# Endogenous Price Zones and Investment Incentives in Electricity Markets: An Application of Multilevel Optimization with Graph Partitioning

Mirjam Ambrosius[1,5], Veronika Grimm[1,5], Thomas Kleinert[2,5], Frauke Liers[2,5], Martin Schmidt[3,5], Gregor Zöttl[4,5]

Abstract. In the course of the energy transition, load and supply centers are growing apart in electricity markets worldwide, rendering regional price signals even more important to provide adequate locational investment incentives. This paper focuses on electricity markets that operate under a zonal pricing market design. For a fixed number of zones, we endogenously derive the optimal configuration of price zones and available transfer capacities on a network in order to optimally govern investment and production decisions in the long run. In a multilevel mixed-integer nonlinear model that contains a graph partitioning problem on the first level, we determine welfare-maximizing price zones and available transfer capacities for a given electricity market and analyze their impact on market outcomes. Using a generalized Benders decomposition approach developed in Grimm et al. (2019) and a problem-tailored scenario clustering for reducing the input data size, we are able to solve the model to global optimality even for large instances. We apply the approach to the German electricity market as an example to examine the impact of optimal zoning on key performance indicators such as welfare, generation mix and locations, or electricity prices. It turns out that even for a small number of price zones, an optimal configuration of zones induces a welfare level that almost approaches the first best.

## 1. Introduction

Following the liberalization of the electricity sector in the late 1990s, different electricity market structures have been established around the world. In Europe, Australia, and India, electricity is nowadays traded at power pools at a uniform price for large market areas—typically a country or a state. Originally, this design was thought to minimize the complexity of the pricing settlement and—from a political perspective—a nationwide uniform electricity price is sometimes considered more acceptable. Over the years, national markets have been interconnected, leading to a system of zonal pricing. In this regime, inter-zonal congestion is considered upon trade, but markets have a uniform price inside each region, regardless of transmission congestion within this market area.

Recent developments, however, challenge the current market configuration, e.g., in Europe. Traditionally, the national energy supply was set up such that load centers were equipped with sufficient regional generation capacity. Therefore, national borders were good approximations of suitable price zones. In recent years, however, the transformation towards a sustainable energy system led to a significant shift of electricity supply centers. This development has repeatedly triggered discussions about new zonal configurations or raises calls for additional zoning within a country in order to better reflect the bottlenecks during spot-market trading that result from increasing divergence of production and consumption centers; cf., e.g., Egerer et al. (2016), ENTSO-E (2018, 2019), European Commission (2015), and Official Journal of the European Union (2019). At least coarse regionally differentiated price signals are considered particularly important in order to achieve an

*Date*: January 17, 2020.
*JEL Classification.* C6, L9.
*Key words and phrases.* Price Zones, Electricity Markets, Investment Incentives, Multilevel Optimization.

appropriate balance between the allocation of generation capacity close to load centers and grid expansion.

In this paper, we address the question of optimal zoning from a long-term perspective, i.e., we ask how to shape (a fixed number of) price zones in order to welfare-optimally govern investment and production incentives. We focus on the German electricity market as an important application. Germany is particularly well suited for such an analysis because the expansion of renewable capacities in the north (wind power) and the south (solar systems) together with the decommissioning of nuclear plants by 2022 and also hard coal and lignite by 2038 at the latest will lead to a severe disintegration of generation and load centers. The problem at hand is complex and requires multilevel modeling of an electricity market: At the first level, the regulator decides on price zones and available transfer capacities (ATCs) from a welfare optimization perspective. At the second level, private firms, being aware of the zonal configuration, invest in generation capacity and trade electricity at the spot market. In case of congestion the TSO has to engage in congestion management (redispatch).

For the analysis of an appropriate multilevel model we build on previous work by the authors (Grimm et al. 2019, 2016a; Kleinert and Schmidt 2019) who have developed a generalized Benders decomposition approach to determine the optimal zonal configuration of an electricity market for a predetermined number of zones. We adapt the approach by Grimm et al. (2019) to our specific setup. In particular, we extend and modify the Benders cuts to maintain correctness of the algorithm in our setup. In addition to previous work, we moreover show how available transfer capacities (ATCs) between zones can be chosen optimally. Finally, in order to solve an instance that reflects the German electricity market adequately, it is necessary to simplify the time series of electricity demand and generation parameters without distorting the incentive effect of price peaks. To that aim, we combine density-based and $k$-means clustering techniques to construct smaller scenario sets that yield computationally more tractable models. Similar ideas have been used in, e.g., Feng and Ryan (2013) and Papavasiliou and Oren (2013) in the context of expansion planning and short-term operation models, respectively.

We derive the optimal zonal configuration of the German market area for two and three zones and compare various key figures, such as welfare, price development, and investments in power plants with two benchmark scenarios that reflect the status quo on the one hand and the first-best system configuration on the other hand. We demonstrate that high welfare gains can already be achieved for suitable ATCs by splitting the market into two optimally configured zones, while the implementation of three or more zones only leads to moderate additional welfare gains. As it turns out, restrictive inter-zonal ATCs at the spot market are beneficial since they amplify locational price signals. Inter-zonal ATCs also influence the optimal zonal configuration: more restrictive inter-zonal ATCs force nodes with high load into zones with a high renewable supply and affect the locations of conventional generators accordingly. A comparison with the results from a nodal pricing system reveals that a zonal configuration based on clusters of nodal prices—which is often used in the literature as a heuristic to assign nodes to price zones—does not correspond to the optimal solution.

In the following, we provide a brief overview of the related literature. The derivation of optimal price zones and the associated ATCs requires a multilevel equilibrium model with graph partitioning, which is a classical problem of discrete mathematics. In general, such multilevel mixed-integer nonlinear models are intractable (Dempe et al. 2015; Lodi et al. 2014) and algorithmically complicated to treat; cf., e.g., Moore and Bard (1990) or Fischetti et al. (2017). Fortunately, the special structure of our multilevel market model allows to derive practically useful solution algorithms. For a similar setup, a generalized Benders decomposition approach has been developed in Grimm et al. (2019) and Kleinert and Schmidt (2019), which we adapt to our specific setup.

Our analysis is based on a series of contributions that develop multilevel electricity market models that are suitable to analyze investment incentives in markets with zonal pricing; cf. Murphy and Smeers (2005) as well as Grimm et al. (2019, 2016a), Grimm and Zöttl (2013), and Kleinert and Schmidt (2019). In order to capture different objectives of the regulator and the firms as well as the different information available to the players upon making their decision, a multilevel structure and tailored solution algorithms are necessary; cf. Grimm et al. (2016a) or Hu and Ralph (2007). The correctness of the proposed methods often hinge upon the uniqueness of the lower-level problems. This has been addressed by Grimm et al. (2017), Krebs et al. (2018), and Krebs and Schmidt (2018). Here, we additionally develop novel tie-breaking rules for resolving possibly occurring multiplicities.

The particular issue of price zones has been investigated in various contributions. Stoft (1997) was among the first to point to the fact that an assessment based on physically congested lines may not lead to a satisfactory outcome as it ignores the effects of loop flows. Egerer et al. (2016), Plancke et al. (2016), and Trepper et al. (2015), among others, examine the effects of price zones that are chosen by educated guesses, taking into account frequent congestion between several regions or price similarities. Other contributions employ heuristics on the basis of nodal prices in order to determine adequate zonal configurations; cf. Breuer and Moser (2014), Burstedde (2012), Walton and Tabors (1996), and Felling and Weber (2017).

Some contributions emphasize the importance of a careful configuration of price zones. Grimm et al. (2016b) show that price zones may increase or decrease welfare, depending on their exact configuration. Furthermore, Jensen et al. (2017) show that suboptimal inter-zonal ATCs might mitigate efficiency gains from zonal pricing.

There is also a small amount of literature that addresses optimal zonal configuration. Bjørndal and Jørnsten (2001) use a five-node example with one congested line to demonstrate that a partition based on nodal prices may not lead to a welfare-maximizing outcome. They develop a mixed-integer nonlinear model (MINLP) to determine the short-run optimal zonal configuration for a given number of zones. However, they do not solve this model on any instance. Grimm et al. (2019) present a long-term equilibrium model to determine a welfare-maximizing zonal configuration and provide problem-tailored solution algorithms. Kleinert and Schmidt (2019) further enhance the model and the solution approach by including optimal network design. The present paper is a follow-up paper of the two latter ones. We adapt the models and solution techniques developed therein, to obtain a quantitative analysis for the German electricity market.

In our study, we also compare the outcome of an optimal zonal configuration to a nodal pricing solution, which corresponds to the first-best solution in our setup. Nowadays nodal pricing is implemented, e.g., in the United States, Argentina, Chile, Ireland, New Zealand, and Russia; cf. Holmberg and Lazarczyk (2015). Several authors point out arguments for zonal and nodal pricing, respectively. It is not the aim of this paper to evaluate the different pricing schemes. For a detailed discussion, see, e.g., Bertsch et al. (2016), Ding and Fuller (2005), and Neuhoff et al. (2013) for arguments in favor of nodal pricing and Holmberg and Lazarczyk (2015), Leuthold et al. (2008) for arguments questioning the benefit of nodal pricing.

The remainder of the paper is organized as follows. In Section 2 we present the model and also provide details on the solution approach. A brief description of the data used to calibrate the model is contained in Section 3—all details are later presented in Appendix A. Section 4 contains the results of the numerical analysis. The paper closes with a summary and concluding remarks in Section 5.

## 2. The Model

In this section, we present the trilevel market model that is an extension of the one used in Grimm et al. (2019). The model reflects the current European electricity market

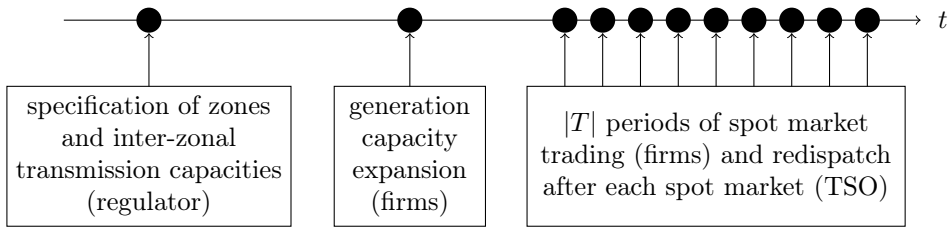


FIGURE 1. Timing of the considered model setup; adapted from Grimm et al. (2019).

design where network restrictions are not fully reflected upon spot-market trading. Figure 1 illustrates a stylized timeline for decision making by the different agents under these market rules. We explain the model in reverse order (i.e., backwards) to better illustrate the incentive structure. At the spot markets, electricity is traded hourly; see the rightmost box under the timeline. At the hourly markets, intra-zonal transfer capacities are neglected, while inter-zonal constraints are taken into account. We assume that inter-zonal capacities (ATCs) are determined in advance on a long-term basis, which is a common approach in the electricity market literature (Fürsch et al. 2013; Gerbaulet and Lorenz 2017; Huppmann and Egerer 2015; Kemfert et al. 2016) and is also done in German transmission planning (German TSOs 2017). In case the quantities traded at the spot market are infeasible on the network, congestion is resolved by the regulated transmission system operator (TSO) via cost-based redispatch—also at an hourly basis. The TSO can take the following measures, which she uses in exactly this order: First, the TSO can instruct power plants in the import-constrained region to start up and instruct plants in the export-constrained region to reduce production. All plants will be compensated exactly for the additional costs that arise due to this redispatch intervention. The TSO will act in such a way that the total costs of the intervention are minimal. If redispatch of the power plants cannot eliminate all infeasibilities, the TSO can take further measures, which we summarize under the term load shedding. In particular, these measures imply that the TSO requests an increase or a decrease in electricity consumption and compensates affected consumers. As in the case of generation redispatch, load shedding is carried out such that load shedding costs are minimized.

Investment in generation capacity (middle box under the timeline) is decided upon by private firms under a profit maximization objective in anticipation of the revenues earned at the spot markets over the lifetime of the respective generation unit.

The welfare optimal configuration of zones, as well as the size of ATCs, are decided by the regulator in anticipation of the behavior at the previously described stages; see the leftmost box under the timeline. Thus, the optimal zonal configuration and size of ATCs take into account the effects on the locational decisions for the power plants upon investment and their production decisions.

In Grimm et al. (2016a) the authors show that this framework can be translated into a multilevel equilibrium model as follows. At the first level, the regulator decides on the specification of price zones and the optimal size of ATCs. The objective of the regulator is to maximize social welfare, anticipating the outcomes at all subsequent levels. Generation investment decisions of private firms and spot-market trading are modeled at the second level. In contrast to the regulator, private firms aim to maximize profits. Spot-market trading takes place on an hourly basis and we assume perfectly competitive firms. Note that the integration of the generation investment and spot-market level is possible only under the assumption of perfect competition. At the third level, cost-based redispatch is carried out by the TSO in order to resolve any congestion that might occur due to spot-market outcomes. The TSO's objective at this level is to minimize redispatch costs.

In order to make this work self-contained, we first introduce the basic notation used in our mathematical model. Then, we explain each level of the model in detail and briefly discuss our solution approach that is an adaption of the methods developed in Grimm et al. (2019). Later, in Section 4, we apply the model and the solution approach to the German electricity market as an example.

2.1. **Basic Economic and Technical Setup.** We consider an electricity transmission network $\mathcal{G} = (N, L)$ with node set $N = N^{\mathrm{dom}} \cup N^{\mathrm{abr}}$, where the sets $N^{\mathrm{dom}}$ and $N^{\mathrm{abr}}$ denote domestic and abroad nodes, respectively, and a set of transmission lines $L \subseteq N \times N$. We further denote the set of lines connecting domestic nodes by $L^{\mathrm{dom}}$ and the set of lines connecting domestic and abroad nodes by $L^{\mathrm{abr}}$, i.e.,

$$L^{\mathrm{dom}} := \{l \in L \colon l = (n, m) \text{ with } n \in N^{\mathrm{dom}},\, m \in N^{\mathrm{dom}}\},$$
$$L^{\mathrm{abr}} := \{l \in L \colon l = (n, m) \text{ with } n \in N^{\mathrm{dom}},\, m \in N^{\mathrm{abr}}\}.$$

Note that there are no lines $l = (n, m)$ with $n \in N^{\mathrm{abr}}$ and $m \in N^{\mathrm{dom}} \cup N^{\mathrm{abr}}$. This means that we consider a directed graph and that there are no lines connecting two neighboring countries with each other. Otherwise, it would be possible to resolve infeasibilities that occur in the German transmission network via loop flows through neighboring countries. There is a political consensus that this should be avoided as far as possible (THEMA Consulting Group 2013). Hence, $L = L^{\mathrm{dom}} \cup L^{\mathrm{abr}}$ holds. We furthermore divide the set of domestic transmission lines $L^{\mathrm{dom}}$ into high-voltage direct current (HVDC) lines $L^{\mathrm{HVDC}}$ and alternating current (AC) lines $L^{\mathrm{AC}}$, i.e., $L^{\mathrm{dom}} = L^{\mathrm{HVDC}} \cup L^{\mathrm{AC}}$. All transmission lines $l \in L$ are characterized by their capacity $\bar{f}_l$ and their susceptance $B_l$. Throughout the paper we use the following notation: the sets of in- and outgoing lines of a node set $N' \subseteq N$ are denoted by $\delta^{\mathrm{in}}_{N'}$ and $\delta^{\mathrm{out}}_{N'}$, respectively. At every node $n \in N$, we introduce a set of consumers $C_n$ (with $0 \leq |C_n| < \infty$) that are located at that node. We further assume a given set of scenarios $T = \{1, \ldots, |T|\}$. Elastic demand of a consumer $c \in C_n$ at node $n \in N$ in scenario $t \in T$ is modeled by a continuous and strictly decreasing inverse demand function $p_{t,c} = p_{t,c}(d_{t,c})$, where $d_{t,c}$ denotes the demand of this consumer. Throughout the paper we make the additional assumption that inverse demand functions are linear and decreasing. In this case, the gross consumer surplus

$$\int_0^{d_{t,c}} p_{t,c}(\omega)\,\mathrm{d}\omega$$

is a strictly concave quadratic function, which is important to obtain a tractable model. We point out that $d_{t,c} \geq 0$ is assumed for domestic consumers located at nodes $n \in N^{\mathrm{dom}}$. However, demand and supply at abroad nodes is aggregated via net export functions.[1] Negative demand $d_{t,c} < 0$ for $n \in N^{\mathrm{abr}}$ is then used to model abroad generation.

We thus introduce finite sets of generators $G^{\mathrm{all}}_n$ at domestic nodes $n \in N^{\mathrm{dom}}$ only. For simplicity, we aggregate all generators of the same technology that are located at the same node. We distinguish between conventional generators $G^{\mathrm{conv}}_n$ and renewable energy sources (RES) $G^{\mathrm{res}}_n$. Conventional generators $G^{\mathrm{conv}}_n$ can be further divided into existing generators $G^{\mathrm{ex}}_n$ that might be dismantled and candidate generators $G^{\mathrm{new}}_n$ that firms can invest in. In summary, $G^{\mathrm{all}}_n = G^{\mathrm{conv}}_n \cup G^{\mathrm{res}}_n = G^{\mathrm{new}}_n \cup G^{\mathrm{ex}}_n \cup G^{\mathrm{res}}_n$ holds. Existing conventional generators $g \in G^{\mathrm{ex}}_n$ have given capacities $\bar{q}^{\mathrm{ex}}_g$. However, private firms may decide to dismantle these capacities partly or completely by $\bar{q}^{\mathrm{dis}}_g$. Firms can also invest in generation capacities $\bar{q}^{\mathrm{new}}_g$ of candidate conventional generators $g \in G^{\mathrm{new}}_n$. All conventional generators are characterized by their operating costs $c^{\mathrm{op}}_g > 0$ and their variable production costs $c^{\mathrm{var}}_g > 0$. Furthermore, candidate generators have investment costs $c^{\mathrm{inv}}_g > 0$ for newly

[1] Considering the net export function of neighboring countries is only an approximation. A more realistic modeling of the interaction with neighboring countries leads to even more complicated models, see Egerer et al. (2019), which is why we refrain from considering these effects in this paper.

installed generation capacity. In contrast, renewable generation capacities are determined exogenously. As a result, operating costs of RES plants are not considered since it would be a constant cost term in the objective function; see below. We explicitly point out that all RES generators have variable costs of zero. For every generator $g \in G_n^{\mathrm{all}}$, $n \in N$, generation quantities are denoted by $q_{t,g}$. In the following we denote demand and production quantities belonging to the spot-market and redispatch level by a super-index "spot" or "rd", respectively. Furthermore, super-indices "ls+" and "ls−" denote quantities of positive and negative load shedding. Let us point out that, although the main modeling is taken from Grimm et al. (2019) and Kleinert and Schmidt (2019), many new details are introduced here to enable a quantitative analysis of the German electricity market—among them the modeling of abroad nodes, renewable generators, dismantling, operational costs, load shedding, and the optimal determination of ATCs.

2.2. **First-Level Problem: Specification of Price Zones and Inter-Zonal Transfer Capacities.** At the first level, in which the regulator seeks to maximize welfare, he decides on the specification of price zones and on the transfer capacities of the network taken into account for inter-zonal trade at the spot markets. Welfare is given by the difference of gross consumer surplus and total system costs, i.e., variable costs of generation (after redispatch), investment and operating, as well as load shedding costs $c^{\mathrm{ls}+}$ and $c^{\mathrm{ls}-}$ for redispatched demand $d_{t,c}^{\mathrm{ls}+}$ or $d_{t,c}^{\mathrm{ls}-}$ of a domestic consumer $c \in C_n$ at node $n \in N^{\mathrm{dom}}$. Thus, the objective reads

$$\begin{aligned}\psi_1 :=& \sum_{t\in T}\sum_{n\in N}\sum_{c\in C_n}\int_0^{d_{t,c}^{\mathrm{rd}}} p_{t,c}(\omega)\,\mathrm{d}\omega - \sum_{t\in T}\sum_{n\in N^{\mathrm{dom}}}\sum_{g\in G_n^{\mathrm{all}}} c_g^{\mathrm{var}} q_{t,g}^{\mathrm{rd}} \\ &- \sum_{n\in N^{\mathrm{dom}}}\left(\sum_{g\in G_n^{\mathrm{new}}}(c_g^{\mathrm{inv}}+c_g^{\mathrm{op}})\bar{q}_g^{\mathrm{new}} + \sum_{g\in G_n^{\mathrm{ex}}} c_g^{\mathrm{op}}(\bar{q}_g^{\mathrm{ex}}-\bar{q}_g^{\mathrm{dis}})\right) \\ &- \sum_{t\in T}\sum_{n\in N^{\mathrm{dom}}}\sum_{c\in C_n}\left(c^{\mathrm{ls}+}d_{t,c}^{\mathrm{ls}+} + c^{\mathrm{ls}-}d_{t,c}^{\mathrm{ls}-}\right).\end{aligned}$$

Note that the regulator may only specify price zones within its country. Each of the neighboring countries is considered as a single separate price zone. According to Grimm et al. (2019), the specification of price zones is modeled as follows. A price zone $Z_i$ is part of a partition of the node set $N^{\mathrm{dom}}$. The number of zones in the partition is set to $k \in \{1,\dots,|N^{\mathrm{dom}}|\}$, where $k$ is given as an input. Consequently, $N^{\mathrm{dom}} = Z_1 \cup \dots \cup Z_k$ holds. For every node $n \in N^{\mathrm{dom}}$ the binary variables $x_{n,i} \in \{0,1\}$ indicate to which zone $i \in [k] = \{1,\dots,k\}$ it belongs, i.e., $x_{n,i} = 1$ if and only if node $n$ belongs to zone $i$. The constraint

$$\sum_{i\in[k]} x_{n,i} = 1 \quad \text{for all } n \in N^{\mathrm{dom}} \tag{1}$$

ensures that every node is located in exactly one zone. Since we model price zones, we are only interested in connected partitions. To model connectivity, we use a multi-commodity flow formulation, where every commodity represents a zone. We therefore specify an artificial sink in every zone by introducing binary variables $z_{n,i} \in \{0,1\}$ with $z_{n,i} = 1$ if and only if node $n$ is the artificial sink of zone $i$. Every zone needs to have exactly one such sink:

$$\sum_{n\in N^{\mathrm{dom}}} z_{n,i} = 1 \qquad \text{for all } i \in [k], \tag{2a}$$

$$z_{n,i} \le x_{n,i} \qquad \text{for all } n \in N^{\mathrm{dom}},\ i \in [k]. \tag{2b}$$

To ensure connectivity, every node of a zone must be able to send some flow to the artificial sink of that zone. For modeling this, we define a bi-directed graph $\mathcal{G}' := (N^{\mathrm{dom}}, A)$ with $A$

consisting of lines $a_1(l) = (n, m)$ and $a_2(l) = (m, n)$ for all $l = (n, m) \in L^{\text{dom}}$. Now let $u^i = (u^i_a)_{a \in A} \geq 0$ be the vector of flows of commodity $i \in [k]$. Then, the constraints

$$\sum_{a \in \delta^{\text{out}}_n} u^i_a \leq M x_{n,i} \qquad \text{for all } n \in N^{\text{dom}},\ i \in [k], \tag{3a}$$

$$\sum_{a \in \delta^{\text{out}}_n} u^i_a - \sum_{a \in \delta^{\text{in}}_n} u^i_a \geq x_{n,i} - M z_{n,i} \qquad \text{for all } n \in N^{\text{dom}},\ i \in [k], \tag{3b}$$

where $M$ is a sufficiently large number, ensure connectivity within zones. Note that the $\delta$-notation in (3) operates on the graph $\mathcal{G}'$ and not on the original graph $\mathcal{G}$. We further note that also other ways of modeling connectivity are possible; cf., e.g., Hojny et al. (2018).

For proper modeling of the zonal spot market (cf. Section 2.3) we further introduce indicator variables for inter-zonal lines signaling whether a line connects nodes of different zones. We introduce binary variables $y_l \in \{0, 1\}$ with $y_l = 1$ if and only if line $l$ is an inter-zonal link. This is modeled by the constraints

$$x_{n,i} - x_{m,i} \leq y_l \qquad \text{for all } l = (n, m) \in L^{\text{dom}}, \tag{4a}$$

$$x_{m,i} - x_{n,i} \leq y_l \qquad \text{for all } l = (n, m) \in L^{\text{dom}}, \tag{4b}$$

$$x_{n,i} + x_{m,i} + y_l \leq 2 \qquad \text{for all } l = (n, m) \in L^{\text{dom}}. \tag{4c}$$

As mentioned before, the regulator also determines the welfare-maximizing value of the inter-zonal ATC factor $\beta$ for domestic inter-zonal lines $l \in L^{\text{dom}}$ with $y_l = 1$. This factor determines the percentage of thermal capacity that is available for domestic inter-zonal flows during spot-market trading; cf. Constraint (10) in the next section. For real-world applications, this value is best modeled as a discrete decision. Hence, the regulator is allowed to choose from a discrete set $\mathcal{B} = \{\beta_1, \dots, \beta_{|\mathcal{B}|}\}$ of such factors. This can be modeled by introducing binary variables $b_j$ for $j = 1, \dots, |\mathcal{B}|$, indicating which value $\beta \in \mathcal{B}$ takes. Hence, $b_j = 1$ if and only if $\beta = \beta_j$. The constraints

$$\sum_{j=1}^{|\mathcal{B}|} b_j = 1, \quad \beta = \sum_{j=1}^{|\mathcal{B}|} \beta_j b_j \tag{5}$$

ensure that $\beta$ takes exactly one value. Note that it is, in principle, also possible to model a separate $\beta$ value for every inter-zonal line and/or every scenario. However, we refrain from this for reasons of computational tractability. Note that by holding $\beta$ constant for each scenario, we rather underestimate the effect of price zones on market performance.

Altogether, we obtain the following first-level problem

$$\max \quad \psi_1 \quad \text{s.t.} \quad (1)\text{–}(5). \tag{6}$$

Model (6) consists of a concave-quadratic objective function and a set of mixed-integer linear constraints, i.e., we are facing a mixed-integer quadratic program (MIQP).

2.3. **Second-Level Problem: Generation Investment and Spot-Market Trading.** At the second level, we model decisions regarding investment in conventional generation capacity and spot-market trading by private firms. These decisions are taken with the goal to maximize individual profits. We assume perfectly competitive markets, i.e., firms perceive market prices as given and independent of their own decisions. Although this might not be the case for power systems in general, this is a common assumption used in the electricity market literature; see, e.g., Boucher and Smeers (2001), Daxhelet and Smeers (2007), and Grimm et al. (2016a). This assumption is important for two reasons: First, it has been shown that without the assumption of perfect competition, unique market equilibria cannot be ensured; cf. Zöttl (2010). Second, Grimm et al. (2017) show for the specific situation under consideration that profit maximizing market outcomes under perfect competition are welfare maximizing—a specialization of the classical results of welfare economics (Arrow and Debreu 1954; Walras 1900). Therefore, the assumption of

perfect competition is important in order to keep the multilevel model both theoretically and computationally tractable. For a more detailed discussion; see Grimm et al. (2016a). During spot-market trading, firms neglect all transmission capacities within a zone but only account for inter-zonal ATCs. When trading electricity across zones, they receive price signals in case of congestion. This means that the traded quantities between two zones cannot exceed the available capacities of the lines connecting these zones. To ensure market clearing, total generation and inflow in zone $i$ must equal total demand plus total outflow in zone $i$. This is modeled by the zonal version of Kirchhoff's first law:

$$d^{\text{spot}}_{t,n} = \sum_{c \in C_n} d^{\text{spot}}_{t,c} \qquad \text{for all } n \in N^{\text{dom}},\ t \in T, \tag{7a}$$

$$q^{\text{spot}}_{t,n} = \sum_{g \in G^{\text{all}}_n} q^{\text{spot}}_{t,g} + q^{\text{exo}}_{t,n} \qquad \text{for all } n \in N^{\text{dom}},\ t \in T, \tag{7b}$$

$$D_{t,i} = \sum_{n \in N^{\text{dom}}} x_{n,i} d^{\text{spot}}_{t,n} \qquad \text{for all } i \in [k],\ t \in T, \tag{7c}$$

$$Q_{t,i} = \sum_{n \in N^{\text{dom}}} x_{n,i} q^{\text{spot}}_{t,n} \qquad \text{for all } i \in [k],\ t \in T, \tag{7d}$$

$$F^{\text{in}}_{t,i} = \sum_{l=(n,m) \in L^{\text{dom}}} (1 - x_{n,i}) x_{m,i} f^{\text{spot}}_{t,l} \qquad \text{for all } i \in [k],\ t \in T, \tag{7e}$$

$$F^{\text{out}}_{t,i} = \sum_{l=(n,m) \in L^{\text{dom}}} x_{n,i} (1 - x_{m,i}) f^{\text{spot}}_{t,l} \qquad \text{for all } i \in [k],\ t \in T, \tag{7f}$$

$$Q_{t,i} + F^{\text{in}}_{t,i} = D_{t,i} + F^{\text{out}}_{t,i} + \sum_{l=(n,m) \in L^{\text{abr}}} f_{t,l} x_{n,i} \qquad \text{for all } i \in [k],\ t \in T. \tag{7g}$$

The parameter $q^{\text{exo}}_{t,n}$ denotes exogenously given generation at domestic nodes. This includes running water, heat-controlled CHP plants, and transit flows from and to neighboring countries. Note that this parameter may also be negative if transit flow to neighboring countries overcompensates all other components. We want to point out that in case of a nodal system, (7g) coincides with Kirchhoff's first law:

$$\sum_{c \in C_n} d^{\text{spot}}_{t,c} + \sum_{l \in \delta^{\text{out}}_n} f^{\text{spot}}_{t,l} = \sum_{g \in G^{\text{all}}_n} q^{\text{spot}}_{t,g} + \sum_{l \in \delta^{\text{in}}_n} f^{\text{spot}}_{t,l} + q^{\text{exo}}_{t,n} \quad \text{for all } n \in N^{\text{dom}},\ t \in T. \tag{8}$$

Since nodes of neighboring countries are considered to be a single price zone each, flow conservation at these nodes simplifies to

$$\sum_{c \in C_n} d^{\text{spot}}_{t,c} = \sum_{l \in \delta^{\text{in}}_n} f^{\text{spot}}_{t,l} \quad \text{for all } t \in T,\ n \in N^{\text{abr}} \tag{9}$$

because of $\delta^{\text{out}}_n = \emptyset$. Inter-zonal flow restrictions are modeled by capacity constraints. For domestic inter-zonal lines, flows are restricted by the thermal capacity scaled with $\beta$, which is a first-level decision of the regulator, i.e.,

$$-\beta \bar{f}_l - (1 - y_l) M \leq f^{\text{spot}}_{t,l} \leq \beta \bar{f}_l + (1 - y_l) M \quad \text{for all } l \in L^{\text{dom}},\ t \in T. \tag{10}$$

Again, $M$ is a sufficiently large number. Flows between domestic nodes and neighboring countries are restricted by trading capacities $\bar{f}^{\text{atc-ex}}_l$ for export and $\bar{f}^{\text{atc-im}}_l$ for import flows. These parameters can be determined based on historical data and are therefore given exogenously, i.e.,

$$-\bar{f}^{\text{atc-im}}_l \leq f^{\text{spot}}_{t,l} \leq \bar{f}^{\text{atc-ex}}_l \quad \text{for all } l \in L^{\text{abr}},\ t \in T. \tag{11}$$

Spot-market generation and demand is modeled by continuous variables $q^{\text{spot}}_{t,g}$ and $d^{\text{spot}}_{t,c}$, respectively. Generation quantities of RES generators $g \in G^{\text{res}}_n$ are bounded by their actual available capacities, which are given by their physical capacity $\bar{q}^{\text{res}}_g$, the power generation

per unit of capacity $\eta_g \in [0,1]$, and weather effects $\alpha_{t,g} \in [0,1]$. We distinguish between must-run generators $G_n^{\mathrm{mr}}$ that always run at full available capacity and generators $G_n^{\mathrm{cur}}$ that can be curtailed whenever this is beneficial, i.e., $G_n^{\mathrm{res}} = G_n^{\mathrm{mr}} \cup G_n^{\mathrm{cur}}$ holds. Spot-market RES generation is thus modeled in the following way:

$$0 \leq q_{t,g}^{\mathrm{spot}} = \eta_g \alpha_{t,g} \bar{q}_g^{\mathrm{res}} \qquad \text{for all } t \in T,\ n \in N^{\mathrm{dom}},\ g \in G_n^{\mathrm{mr}}, \tag{12a}$$

$$0 \leq q_{t,g}^{\mathrm{spot}} \leq \eta_g \alpha_{t,g} \bar{q}_g^{\mathrm{res}} \qquad \text{for all } t \in T,\ n \in N^{\mathrm{dom}},\ g \in G_n^{\mathrm{cur}}. \tag{12b}$$

Existing conventional generation plants can only be dismantled up to the existing capacity. Possible production capacities of conventional generators $g \in G_n^{\mathrm{conv}}$ are determined by physical capacities and power generation per unit of capacity $\eta_g \in [0,1]$. Consequently, we have

$$0 \leq \bar{q}_g^{\mathrm{dis}} \leq \bar{q}_g^{\mathrm{ex}} \qquad \text{for all } n \in N^{\mathrm{dom}},\ g \in G_n^{\mathrm{ex}}, \tag{13a}$$

$$0 \leq q_{t,g}^{\mathrm{spot}} \leq \eta_g \left(\bar{q}_g^{\mathrm{ex}} - \bar{q}_g^{\mathrm{dis}}\right) \qquad \text{for all } t \in T,\ n \in N^{\mathrm{dom}},\ g \in G_n^{\mathrm{ex}}. \tag{13b}$$

For some technologies (e.g., market-controlled CHP plants), the maximum capacity of newly built generators per node is restricted. This can be due to technical or political reasons. As for each node all generators of the same technology are aggregated, this restriction can be simplified to a constraint concerning the maximum newly built capacity $\bar{q}_g^{\max}$ per generator. It can also be the case for some specified subsets $\tilde{G} \subset \mathcal{P}(G)$, $G := \cup_{n \in N} G_n^{\mathrm{all}}$, that newly built capacity is restricted globally. Here, $\mathcal{P}(G)$ denotes the respective power set. This means that the sum of all investments in this technology across all nodes cannot exceed a given amount $\bar{q}_{\tilde{G}}^{\max}$. Hence, we need the following constraints to model candidate generation of conventional generators:

$$0 \leq q_{t,g}^{\mathrm{spot}} \leq \eta_g \bar{q}_g^{\mathrm{new}} \qquad \text{for all } t \in T,\ n \in N^{\mathrm{dom}},\ g \in G_n^{\mathrm{new}}, \tag{14a}$$

$$0 \leq \bar{q}_g^{\mathrm{new}} \leq \bar{q}_g^{\max} \qquad \text{for all } n \in N^{\mathrm{dom}},\ g \in G_n^{\mathrm{new}}, \tag{14b}$$

$$\sum_{g \in G'} \bar{q}_g^{\mathrm{new}} \leq \bar{q}_{G'}^{\max} \qquad \text{for all } G' \in \tilde{G}. \tag{14c}$$

Finally, we impose simple variable bounds for domestic spot-market demands by

$$0 \leq d_{t,c}^{\mathrm{spot}} \quad \text{for all } t \in T,\ n \in N^{\mathrm{dom}},\ c \in C_n. \tag{15}$$

To summarize, at level two we consider welfare-maximizing generation investment and dismantling as well as production and demand decisions, i.e., the objective function $\psi_2$ of the second level is given by

$$\begin{aligned}\psi_2 :=& \sum_{t \in T} \sum_{n \in N} \sum_{c \in C_n} \int_0^{d_{t,c}^{\mathrm{spot}}} p_{t,c}(\omega)\, \mathrm{d}\omega - \sum_{t \in T} \sum_{n \in N^{\mathrm{dom}}} \sum_{g \in G_n^{\mathrm{all}}} c_g^{\mathrm{var}} q_{t,g}^{\mathrm{spot}} \\ & - \sum_{n \in N^{\mathrm{dom}}} \left( \sum_{g \in G_n^{\mathrm{new}}} (c_g^{\mathrm{inv}} + c_g^{\mathrm{op}}) \bar{q}_g^{\mathrm{new}} + \sum_{g \in G_n^{\mathrm{ex}}} c_g^{\mathrm{op}} (\bar{q}_g^{\mathrm{ex}} - \bar{q}_g^{\mathrm{dis}}) \right).\end{aligned}$$

The second-level problem thus reads

$$\max \quad \psi_2 \quad \text{s.t.} \quad (7), (9)\text{–}(15).$$

By linearization of the zonal version of Kirchhoff's first law (7), we obtain a concave-quadratic maximization problem over mixed-integer linear constraints, in which all discrete variables are decided upon at the first level.

2.4. **Third-Level Problem: Cost-Optimal Redispatch.** At the third level, the TSO resolves network congestion via cost-based redispatch of generation and load shedding, where the latter is only applied in case that generation redispatch cannot resolve spot-market infeasibilities.[2] We assume that any congestion needs to be resolved within the country, i.e., load shedding is only carried out for domestic consumers. Demand quantities after redispatch $d^{\mathrm{rd}}_{t,c}$ are composed of spot-market demand and positive or negative load shedding, $d^{\mathrm{ls}+}_{t,c}, d^{\mathrm{ls}-}_{t,c} \geq 0$, respectively and are defined as follows:

$$d^{\mathrm{rd}}_{t,c} = d^{\mathrm{spot}}_{t,c} + d^{\mathrm{ls}+}_{t,c} - d^{\mathrm{ls}-}_{t,c} \qquad \text{for all } t \in T,\ n \in N^{\mathrm{dom}},\ c \in C_n,$$
$$d^{\mathrm{rd}}_{t,c} = d^{\mathrm{spot}}_{t,c} \qquad \text{for all } t \in T,\ n \in N^{\mathrm{abr}},\ c \in C_n.$$

We impose costs $c^{\mathrm{ls}+}, c^{\mathrm{ls}-} > 0$ for positive and negative load shedding, which represent the value of lost load.[3] Note that due to strictly positive costs for load shedding, the variables determining positive and negative load shedding will never be positive at the same time for the same consumer. Cost-minimizing redispatch is carried out in order to ensure feasibility with respect to transmission constraints. Redispatch costs are given by

$$\psi_3 := \sum_{t\in T}\sum_{n\in N^{\mathrm{dom}}} \left( \sum_{c\in C_n} \int_{d^{\mathrm{rd}}_{t,c}}^{d^{\mathrm{spot}}_{t,c}} p_{t,c}(\omega)\,\mathrm{d}\omega + \sum_{g\in G^{\mathrm{all}}_n} c^{\mathrm{var}}_g \left(q^{\mathrm{rd}}_{t,g} - q^{\mathrm{spot}}_{t,g}\right) \right)$$
$$+ \sum_{t\in T}\sum_{n\in N^{\mathrm{dom}}} \left( \sum_{c\in C_n} \left(c^{\mathrm{ls}+} d^{\mathrm{ls}+}_{t,c} + c^{\mathrm{ls}-} d^{\mathrm{ls}-}_{t,c}\right) \right).$$

Redispatch has to account for all physical transmission constraints. Besides Kirchhoff's first law (8), this includes Kirchhoff's second law that determines the voltage angles $\theta_{t,n}$, $t \in T$, $n \in N$, in the network and is modeled via a DC-lossless approach as given in Stigler and Todem (2005):

$$f^{\mathrm{rd}}_{t,l} = B_l(\theta_{t,n} - \theta_{t,m}) \quad \text{for all } l = (n,m) \in L \setminus L^{\mathrm{HVDC}},\ t \in T. \tag{16}$$

Note that Kirchhoff's second law only applies to AC lines. This is due to the full controllability of power flow in HVDC lines as opposed to AC transmission. While power flow in AC lines is based on Kirchhoff's law, and thus depends on the entire network topology and all impedances, required power flow in HVDC lines can be controlled simply by adjusting the converter valves; see, e.g., Wang et al. (2008) or van der Weijde and Hobbs (2012). We further fix the voltage angle at an arbitrary node $\hat{n} \in N$ for every time period in order to obtain unique physical solutions:

$$\theta_{t,\hat{n}} = 0 \quad \text{for all } t \in T. \tag{17}$$

Furthermore, all transmission flows are limited by physical or trading capacities, i.e.,

$$-\bar{f}_l \leq f^{\mathrm{rd}}_{t,l} \leq \bar{f}_l \qquad \text{for all } l \in L^{\mathrm{dom}},\ t \in T, \tag{18a}$$
$$-\bar{f}^{\text{atc-im}}_l \leq f^{\mathrm{rd}}_{t,l} \leq \bar{f}^{\text{atc-ex}}_l \qquad \text{for all } l \in L^{\mathrm{abr}},\ t \in T. \tag{18b}$$

Thus, the third-level problem reads

$$\min \quad \psi_3 \quad \text{s.t.} \quad (8), (12), (13b), (14a), (15)\text{–}(18),$$

where we replaced $d^{\mathrm{spot}}_{t,n}, q^{\mathrm{spot}}_{t,g}, f^{\mathrm{spot}}_{t,l}$ in (8)–(15) by the redispatch variables $d^{\mathrm{rd}}_{t,n}, q^{\mathrm{rd}}_{t,g}, f^{\mathrm{rd}}_{t,l}$. We obtain a convex-quadratic minimization problem over linear constraints.

2.5. **Model Discussion and Solution Approach.** The entire trilevel market model is shown in Figure 2. This model is a mixed-integer trilevel optimization model that is very hard both in theory and in practice. In order to tackle instances of relevant size,

[2] Note that this is in line with § 13.2 of the German Industry Act; see EnWG (2005).

[3] The fact that load shedding is only considered if generation redispatch does not suffice is modeled implicitly via imposing penalty costs in the objective function that are not considered for the welfare-analysis.

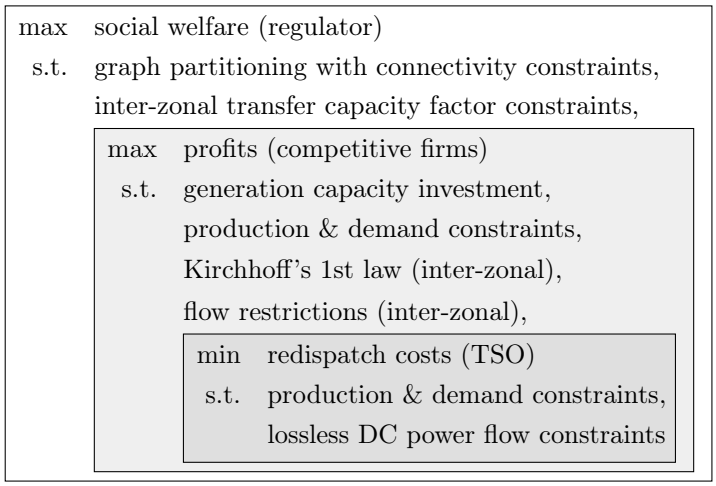


FIGURE 2. Structure of the trilevel market model; adapted from Grimm et al. (2019).

problem-tailored solution approaches need to be used. Fortunately, the model has a special structure that we can exploit: Level one depends on the variables of levels two and three, whereas level two only depends on the discrete variables of the first level, and level three depends on continuous variables of the second level. This weak coupling can be exploited by tailored decomposition methods. Grimm et al. (2019) propose a generalized Benders decomposition for a similar model with the same structure. In their computational study they demonstrate that this approach is superior to a single-level Karush–Kuhn–Tucker (KKT) reformulation. Hence, we use their approach with a slightly adjusted Benders optimality cut that ensures correctness of the method in our extended framework. In particular, the cut also needs to account for first-level decisions on inter-zonal transfer capacities. The approach decomposes all three levels and the problem can thus be solved in an iterative way. In each iteration, a master problem provides a certain zoning and an ATC factor. Then, for this solution the spot-market and subsequently the redispatch model is solved.

The correctness of this method heavily relies on the uniqueness of the redispatch model. Since the redispatch model is determined by spot-market quantities, unique spot-market solutions are desirable. Grimm et al. (2017) establish conditions under which uniqueness of spot-market equilibria is obtained. Among others, it is necessary that all variable production costs are pairwise distinct. This is not the case for most conventional production, as variable production costs often do not differ within a technology group. Economically, this means that when determining the optimal production or capacity investment decisions, one might be indifferent between two or more generators with the same investment and variable production cost located in the same price zone.

To establish uniqueness of spot-market outcomes in our model, we implement the following tie-breaking rules. Whenever a group of generation technologies in the same price zone has the same investment and variable cost, the total amount of investment, dismantling and production for this group is divided up equally (proportional to their respective upper bound for investment, dismantling and production) between all generators of this group. More formally, our tie-breaking rules can be described as follows. Let $G^e \subseteq G$, $e \in E$, be the set of all generators with equal variable production and investment or operational cost. First, investment in generation capacity and dismantling need to be determined via

tie-breaking for the generator groups $G^e$. This is done by the following rules:

$$(\bar{q}_g^{\text{new}})^* = r_{i,e}^{\text{inv}} \bar{q}_g^{\max} \qquad \text{for all } g \in G_n^{\text{new}} \cap G^e,\ n \in Z_i,\ i \in [k],$$
$$\bar{q}_g^{\text{ex}} - (\bar{q}_g^{\text{dis}})^* = r_{i,e}^{\text{inv}} \bar{q}_g^{\text{ex}} \qquad \text{for all } g \in G_n^{\text{ex}} \cap G^e,\ n \in Z_i,\ i \in [k],$$

where $r_{i,e}^{\text{inv}}$ denotes the ratio of capacity investment with respect to the maximum possible investment for a given zone and technology. In this context, remaining existing capacity, which is not dismantled, is interpreted as an investment with investment costs $c_g^{\text{op}}$. Hence, $r_{i,e}^{\text{inv}}$ is given by

$$r_{i,e}^{\text{inv}} = \frac{\sum_{n \in Z_i} \left( \sum_{g \in G_n^{\text{new}} \cap G^e} \bar{q}_g^{\text{new}} + \sum_{g \in G_n^{\text{ex}} \cap G^e} \left( \bar{q}_g^{\text{ex}} - \bar{q}_g^{\text{dis}} \right) \right)}{\sum_{n \in Z_i} \left( \sum_{g \in G_n^{\text{new}} \cap G^e} \bar{q}_g^{\max} + \sum_{g \in G_n^{\text{ex}} \cap G^e} \bar{q}_g^{\text{ex}} \right)} \quad \text{for all } i \in [k],\ e \in E,$$

where the quantities $\bar{q}_g^{\text{new}}$ and $\bar{q}_g^{\text{dis}}$ belong to an optimal second-level solution.

Total spot-market generation of all generators $g \in G_n^e$ of generator set $e \in E$ in zone $i$ is divided up proportionally to available generation capacity:

$$(q_{t,g}^{\text{spot}})^* = r_{t,i,e}^{\text{gen}} \eta_g (\bar{q}_g^{\text{ex}} - \bar{q}_g^{\text{dis}}) \quad \text{for all } g \in G_n^{\text{ex}} \cap G^e,\ n \in Z_i,\ i \in [k],\ t \in T,$$

and

$$(q_{t,g}^{\text{spot}})^* = r_{t,i,e}^{\text{gen}} \eta_g \bar{q}_g^{\text{new}} \quad \text{for all } g \in G_n^{\text{new}} \cap G^e,\ n \in Z_i,\ i \in [k],\ t \in T.$$

Here, $r_{t,i,e}^{\text{gen}}$ denotes the total load factor of conventional generation for group $e$ of generators with equal production and investment or operational cost for a given zone $i$ and scenario $t$, i.e.,

$$r_{t,i,e}^{\text{gen}} = \frac{\sum_{n \in Z_i} \sum_{g \in (G_n^{\text{ex}} \cup G_n^{\text{new}}) \cap G^e} q_{t,g}^{\text{spot}}}{\sum_{n \in Z_i} \left( \sum_{g \in G_n^{\text{ex}} \cap G^e} \eta_g (\bar{q}_g^{\text{ex}} - \bar{q}_g^{\text{dis}}) + \sum_{g \in G_n^{\text{new}} \cap G^e} \eta_g \bar{q}_g^{\text{new}} \right)}$$

for all $i \in [k]$, $t \in T$, and $e \in E$. Again, $q_{t,g}^{\text{spot}}$ belongs to an optimal second-level solution.

2.6. **The Integrated Planner Model.** We additionally consider a model in which all decisions regarding investment and dismantling as well as production and demand are taken simultaneously by a fictitious integrated generation and transmission company (IGTC) that aims to maximize the social welfare $\psi_{\text{IGTC}}$. This is a standard approach to determine the system optimum that serves as a first-best benchmark; cf., e.g., Powell and Oren (1989). In the following, social welfare is defined—as usual—as the difference of gross consumer surplus and generation capacity investment costs as well as variable costs of production and operational costs:

$$\begin{aligned} \psi_{\text{IGTC}} := & \sum_{t \in T} \sum_{n \in N} \sum_{c \in C_n} \int_0^{d_{t,c}} p_{t,c}(\omega)\, \mathrm{d}\omega - \sum_{t \in T} \sum_{n \in N^{\text{dom}}} \sum_{g \in G_n^{\text{all}}} c_g^{\text{var}} q_{t,g} \\ & - \sum_{n \in N^{\text{dom}}} \left( \sum_{g \in G_n^{\text{new}}} (c_g^{\text{inv}} + c_g^{\text{op}}) \bar{q}_g^{\text{new}} + \sum_{g \in G_n^{\text{ex}}} c_g^{\text{op}} (\bar{q}_g^{\text{ex}} - \bar{q}_g^{\text{dis}}) \right). \end{aligned}$$

The integrated planner has to account for generation and demand constraints, as well as for the full physical network, i.e., the integrated planner model is given by

$$\begin{aligned} \max \quad & \psi_{\mathrm{IGTC}} \\ \text{s.t.} \quad & \text{Kirchhoff's first law: (8)}, \\ & \text{RES capacity constraints: (12)}, \\ & \text{Generation capacity constraints: (13), (14)}, \\ & \text{Demand bounds: (15)}, \\ & \text{Kirchhoff's second law: (16), (17)}, \\ & \text{Transmission flow limits: (18)}, \end{aligned}$$

where we replaced spot-market and redispatch quantities by the corresponding integrated planner quantities $d_{t,c}$, $q_{t,g}$, $f_{t,l}$. In summary, the integrated planner model is a continuous maximization problem with linear constraints and a concave-quadratic objective function.

## 3. Data

To illustrate the capability of our approach, we apply the model to a simplified representation of the German market area. The plan of the German government to push ahead with a comprehensive energy system transformation qualifies the country as the subject of our case study. In particular, extensive data and scenarios exist which form the basis for the calibration of our model. We briefly outline the data basis taken for our computations in this section. A comprehensive overview of all relevant data can be found in Appendix A.

The data for the calibration of the model for the German electricity market is mainly based on the data of the German Network Development Plan (NDP) 2030 (version 2017); cf. German TSOs (2017). In particular, we consider a scenario for the year 2035, called B 2035.

For our purposes we use an aggregation of the German electricity network into 28 nodes—one node per federal state and twelve nodes for the neighboring countries. All physical parameters and the underlying alternating current transmission network are taken from data provided by the four German TSOs and Egerer et al. (2014). We do not consider line investment endogenously but focus on two different line investment scenarios. The first scenario is taken from NDP 2014 (German TSOs 2014a) and assumes that all 15 line candidates proposed in German TSOs (2014a) are actually built in 2035. The second scenario considers a significantly smaller amount of network expansion of only five lines that are proposed in German TSOs (2017).

Assumptions concerning existing generation capacities in 2035 are based on the power plant list published in German TSOs (2017). As existing power plants in 2035, we consider all power plants that are currently installed and will not be dismantled in the foreseeable future as well as those that are already under construction. Investment in conventional generation capacity is determined endogenously in our model for gas turbines, combined cycle gas turbines, and market-controlled CHP generators. Note that we do not allow for investment in lignite and coal generators, but only for dismantling of already existing capacity due to current efforts towards a coal phase-out in Germany; cf., e.g., Gerbaulet et al. (2012). Investment, operating, and production costs of conventional generation are taken from Konstantin (2013). Since we consider a one-year time horizon, we use annuities where appropriate.

Installed capacities of renewable generators are exogenously given in our model. We rely on the predicted installed capacities and locations from scenario B 2035 in German TSOs (2017). Variable cost of production for all RES generators is assumed to be zero. We also include electricity flows from running water, heat-controlled CHP plants, and transit flows from neighboring European countries through Germany. These flows are assumed to be exogenous and independent of spot-market prices and market design. Running water

power flows are included as an hourly vector that is computed using the data from Destatis (2016a) and BDEW (2015). Generation of heat-controlled CHP plants is assumed to be constant over time. We use the estimations in EnCN/FAU/Prognos (2016). Transit flows are taken from German TSOs (2017).

To calibrate hourly demand functions we use observations for 2014 taken from `www.entsoe.eu`. In line with German TSOs (2014a), we assume that net electricity demand remains constant until 2035. The reason is that German TSOs (2014a) assume that future efficiency gains are balanced by a growing demand induced by, e.g., electricity demand for heating or e-mobility. This leads to 8760 hourly demand values that need to be considered together with hourly RES production on the second level. In order to reduce computation times, we apply scenario reduction techniques, which are often applied in capacity expansion models; cf., e.g., Feng and Ryan (2013) and Papavasiliou and Oren (2013). In a quite similar framework to ours, Lara et al. (2018) analyze the long-term planning of electric power infrastructures in the context of high renewable penetration. In particular, their model incorporates annual generation investment decisions and hourly operational decisions within a multi-year planning horizon. They apply a $k$-means clustering algorithm (Arthur and Vassilvitskii 2007) to hourly loads and capacity factor profiles to obtain representative days of each year. We use a slightly adopted approach. A $k$-means clustering in general is smoothing out outliers in a way that can distort the results in peak-load-pricing models. Thus, we first apply a density-based clustering to detect outlier scenarios; cf. Ester et al. (1996). All scenarios that cannot be assigned to any cluster are regarded as outliers and are included in our data set. In a second step, we apply a $k$-means algorithm to cluster the remaining non-outlier scenarios. For each cluster obtained we then choose the scenario closest to the cluster center with respect to the Euclidean norm in feature space and weigh it with the respective cluster size. All clustering techniques are carried out using scikit-learn, a machine learning package for Python; see Pedregosa et al. (2011). We tested the entire clustering approach on smaller instances to obtain parameterizations for the involved methods so that both optimal objective function value as well as the optimal solution of the trilevel model are approximated well while simultaneously reducing the problem size as much as possible. With the described approach, we are able to reduce our scenario set from 8760 hourly demand and RES production values to 1248 representative scenarios, which equals the number of hours of one day per week of a year and which corresponds to a reduction of factor $\sim 7$. Our preliminary numerical experiments on smaller instances show that this reduction significantly reduces computation times while yielding to qualitatively similar results compared to the original scenario set.

## 4. Results

In this section, we discuss computational results for the German electricity market. We consider two line expansion scenarios. The first scenario assumes that only five lines are installed, which have been proposed in German TSOs (2017), and are already planned and implemented in concrete terms in Germany. The second scenario is taken from German TSOs (2014a), and assumes that the network is expanded by 15 lines, which would essentially almost completely eliminate congestion issues in the transmission grid. For both scenarios, we compute

(i) the market outcomes for the case without market splitting,
(ii) the optimal zonal configuration and inter-zonal ATC size together with the respective market outcomes in case of two, three, and 16 price zones

For (ii), we consider the set of ATC factors $\mathcal{B} := \{0.25, 0.5, 0.75, 1\}$. We refrain from a finer granularity of $\mathcal{B}$ due to computational reasons. Since we explicitly want to study the economic effects of setting different ATC factors $\beta \in \mathcal{B}$, we not only discuss the optimal value for $\beta$, but also values that are not welfare maximizing. To obtain a first-best benchmark, we further compute

(iii) the market outcome of the integrated planner model, i.e., the first-best benchmark, for the scenario with five new lines.[4]

We refer to scenarios in the following way:

$$[\text{number of new lines - number of zones - } \beta].$$

That is, a scenario with five new transmission lines, two zones, and $\beta = 0.25$ is denoted by [5-2-0.25]. The reference point for our scenario analysis is scenario [5-1-1.0] which we will call status quo in the following.

To compare market outcomes of the different scenarios, we compute various key indicators, which we specify in the following. We first determine, for each zone $i$, the average spot-market price per MWh consumed,

$$p_i^{\text{avg}} = \frac{\sum_{t\in T}\sum_{n\in Z_i}\sum_{c\in C_n} p_{t,i} d_{t,c}^{\text{rd}}}{\sum_{t\in T}\sum_{n\in Z_i}\sum_{c\in C_n} d_{t,c}^{\text{rd}}} \quad \text{for all } i \in [k].$$

The average spot-market price of the entire market (i.e., across all zones) is given by

$$p^{\text{avg}} = \frac{\sum_{t\in T}\sum_{i\in[k]}\sum_{n\in Z_i}\sum_{c\in C_n} p_{t,i} d_{t,c}^{\text{rd}}}{\sum_{t\in T}\sum_{i\in[k]}\sum_{n\in Z_i}\sum_{c\in C_n} d_{t,c}^{\text{rd}}}.$$

For scenarios with more than one zone, we also calculate the maximum spread between average zonal prices, i.e.,

$$\Delta p^{\text{avg}} = \max_{i\in[k]}\{p_i^{\text{avg}}\} - \min_{i\in[k]}\{p_i^{\text{avg}}\}.$$

Finally, we consider the maximum price difference between zones over the entire time horizon:

$$\Delta p^{\max} = \max_{t\in T}\left\{\max_{i\in[k]}\{p_{t,i}\} - \min_{i\in[k]}\{p_{t,i}\}\right\}.$$

Under zonal pricing, the TSO receives payments from congestion pricing and has expenses such as redispatch costs or higher costs for transmission investment, which can substantially differ for different market designs, and which are typically added to the price that consumers pay for electricity. Therefore, it is not meaningful to merely compare spot-market prices of different scenarios in order to assess economic performance of the different market designs. Instead, additional price components such as (i) network fees that are used to pay for congestion management, (ii) transmission line investment and maintenance, and (iii) RES fees that are collected in order to ensure profitability of RES plants should be taken into account.

The network fee allocates the TSO's costs to the customers proportionally to their consumption (per MWh). The TSO's costs are comprised of costs for maintenance $E^{\text{m}}$ of the existing transmission network, annuities of investment costs for existing lines $E^{\text{inv}}$ and congestion management costs or benefits $E^{\text{cm}}$. Congestion management costs are given by the sum of redispatch costs for conventional generators and load shedding costs:

$$E^{\text{cm}} = \sum_{t\in T}\sum_{n\in N^{\text{dom}}}\left(\sum_{g\in G_n^{\text{all}}} c_g^{\text{var}}\left(q_{t,g}^{\text{rd}} - q_{t,g}^{\text{spot}}\right) + \sum_{c\in C_n}\left(c^{\text{ls}+} d_{t,c}^{\text{ls}+} + c^{\text{ls}-} d_{t,c}^{\text{ls}-}\right)\right).$$

Furthermore, the TSO receives revenues $R^{\text{net}}$ from trade across zones in case of congestion since she collects the price differences, i.e.,

$$R^{\text{net}} = \sum_{l=(n,m)\in L}\sum_{t\in T}\left(p_{t,n} - p_{t,m}\right) f_{t,l}.$$

[4]In terms of welfare the integrated planner solution for 15 lines performs much worse, so that we omit it.

Network fees $F^{\text{net}}$ are then determined as the difference of all expenditures and revenues of the TSO divided by total demand:

$$F^{\text{net}} = \frac{E^{\text{m}} + E^{\text{inv}} + E^{\text{cm}} - R^{\text{net}}}{\sum_{t\in T}\sum_{n\in N} d_{t,n}}.$$

Finally, renewable generators (which account for a significant share of electricity production in Germany) need subsidies since investment costs are typically not covered by spot-market revenues. The subsidy is financed by a fee, which is levied on the consumers in proportion to the MWh consumed. We therefore calculate the minimum RES fee $F^{\text{res}}$ that has to be collected to ensure profitability of RES plants. The fee is determined as the difference between total RES investment costs $E^{\text{res}}$ and total revenues from selling RES electricity at the market, which is divided by total demand,

$$F^{\text{res}} = \sum_{n\in N^{\text{dom}}} \frac{E^{\text{res}} - \sum_{t\in T}\sum_{g\in G_n^{\text{res}}} p_{t,n} q_{t,g}^{\text{spot}}}{\sum_{t\in T} d_{t,n}}.$$

Adding a network fee and a RES fee to the load-weighted average zonal spot price yields the corrected average spot price per zone, i.e.,

$$p_i^{\text{corr}} = p_i^{\text{avg}} + F^{\text{net}} + F^{\text{res}}.$$

For countrywide comparisons between scenarios, we also consider the average corrected spot-market price of the entire market,

$$p^{\text{corr}} = p^{\text{avg}} + F^{\text{net}} + F^{\text{res}}.$$

Note that although the corrected average price is an accurate measure of price differences between scenarios, it does not reflect the consumer's electricity price, which is substantially higher due to taxes and further levies.

To compare total social welfare between different scenarios, we use

$$\begin{aligned} W = &\sum_{t\in T}\sum_{n\in N}\sum_{c\in C_n}\int_0^{d_{t,c}^{\text{rd}}} p_{t,c}(\omega)\,\mathrm{d}\omega - \sum_{t\in T}\sum_{n\in N^{\text{dom}}}\sum_{g\in G_n^{\text{all}}} c_g^{\text{var}} q_{t,g}^{\text{rd}} \\ &- \sum_{n\in N^{\text{dom}}}\left(\sum_{g\in G_n^{\text{new}}}(c_g^{\text{inv}} + c_g^{\text{op}})\bar{q}_g^{\text{new}} + \sum_{g\in G_n^{\text{ex}}} c_g^{\text{op}}(\bar{q}_g^{\text{ex}} - \bar{q}_g^{\text{dis}})\right) - E^{\text{inv}} - E^{\text{res}}, \end{aligned}$$

which is the first-level objective function without load shedding costs and with subtracted line investment costs and costs of investments in renewables.

4.1. **Welfare.** Table 1 presents an overview of the main market outcomes for the different scenarios. First, note that the maximum possible welfare gain in our context is determined by the welfare achieved in the first-best scenario as compared to status quo, which is a welfare gain of 1210 million €. Second, we find that all scenarios in which the network is expanded by 15 lines always yield welfare losses as compared to the status-quo scenario. This is mainly due to the high network investment costs which are reflected in a considerable network fee; see column $F^{\text{net}}$. Furthermore, for scenarios with substantial network expansion, the implementation of price zones is ineffective, which is reflected in the moderate price differences across zones; see the last three columns of Table 1. We therefore do not discuss these scenarios in further detail in the following.

Now consider those scenarios where the network is expanded by five transmission lines. In this case, all market splitting scenarios lead to welfare gains as compared to the status quo. It is noticeable that implementing two or three optimally configured price zones with very restrictive inter-zonal ATCs already leads to substantial welfare gains that are relatively close to the welfare gains form the first-best scenario. The highest welfare gain of all considered scenarios can be realized with the implementation of three zones and

TABLE 1. Welfare and prices. We abbreviate the number of candidate lines with $\ell$.

| Scenario | | | $\Delta W$ | $p^{\text{avg}}$ | $F^{\text{net}}$ | $F^{\text{res}}$ | $p^{\text{corr}}$ | $\Delta p^{\text{avg}}$ | $\max\Delta p$ | $d^{\text{redi}}$ |
|---|---|---|---|---|---|---|---|---|---|---|
| $\ell$ | $k$ | $\beta$ | (M€) | (€/MWh) | (€/MWh) | (€/MWh) | (€/MWh) | (€/MWh) | (€/MWh) | (TWh) |
| 5 | 1 | 1.00 | 0 | 50.03 | 15.82 | 9.27 | 75.12 | 0.00 | 0.00 | 542 |
| 5 | 2 | 1.00 | 508 | 50.48 | 12.02 | 9.52 | 72.02 | 2.62 | 47.45 | 544 |
| 5 | 2 | 0.75 | 717 | 50.12 | 11.31 | 8.74 | 70.16 | 0.00 | 2.94 | 546 |
| 5 | 2 | 0.50 | 717 | 53.59 | 5.86 | 12.48 | 71.94 | 22.51 | 141.03 | 542 |
| 5 | 2 | 0.25 | 1007 | 51.71 | 6.79 | 9.54 | 68.05 | 15.34 | 115.59 | 544 |
| 5 | 3 | 1.00 | 700 | 50.50 | 11.06 | 9.33 | 70.89 | 2.62 | 47.45 | 545 |
| 5 | 3 | 0.75 | 795 | 51.67 | 9.21 | 10.52 | 71.40 | 9.86 | 82.56 | 544 |
| 5 | 3 | 0.50 | 885 | 53.62 | 5.34 | 12.43 | 71.39 | 22.51 | 141.03 | 542 |
| 5 | 3 | 0.25 | 1036 | 51.81 | 6.43 | 9.96 | 68.20 | 26.45 | 164.27 | 545 |
| 5 | 16 | 1.00 | 674 | 50.65 | 11.18 | 9.36 | 71.18 | 3.00 | 47.45 | 545 |
| 5 | 16 | 0.75 | 795 | 52.11 | 9.18 | 10.65 | 71.93 | 12.85 | 110.65 | 543 |
| 5 | 16 | 0.50 | 963 | 54.20 | 4.70 | 12.92 | 71.81 | 31.60 | 167.92 | 541 |
| 5 | 16 | 0.25 | 729 | 54.41 | 1.09 | 15.03 | 70.53 | 50.14 | 176.91 | 540 |
| 15 | 1 | 1.00 | −510 | 50.20 | 11.08 | 7.13 | 68.41 | 0.00 | 0.00 | 548 |
| 15 | 2 | 1.00 | −502 | 50.26 | 11.05 | 7.15 | 68.46 | 0.27 | 38.18 | 548 |
| 15 | 2 | 0.75 | −502 | 50.30 | 11.00 | 7.32 | 68.62 | 0.57 | 39.79 | 548 |
| 15 | 2 | 0.50 | −502 | 50.23 | 11.05 | 7.15 | 68.43 | 0.13 | 27.19 | 548 |
| 15 | 2 | 0.25 | −502 | 50.25 | 11.05 | 7.16 | 68.45 | 0.36 | 39.18 | 548 |
| 15 | 3 | 1.00 | −502 | 50.26 | 11.05 | 7.15 | 68.46 | 0.27 | 38.18 | 548 |
| 15 | 3 | 0.75 | −502 | 50.30 | 11.00 | 7.32 | 68.62 | 0.57 | 39.79 | 548 |
| 15 | 3 | 0.50 | −502 | 50.30 | 11.01 | 7.27 | 68.58 | 0.61 | 38.18 | 548 |
| 15 | 16 | 1.00 | −503 | 50.26 | 11.05 | 7.15 | 68.46 | 0.27 | 38.18 | 548 |
| 15 | 16 | 0.75 | −512 | 50.94 | 10.93 | 7.30 | 69.17 | 2.84 | 72.01 | 547 |
| 15 | 16 | 0.50 | −636 | 52.95 | 10.02 | 9.64 | 72.61 | 15.03 | 153.39 | 543 |
| 15 | 16 | 0.25 | −1121 | 54.56 | 6.80 | 14.06 | 75.41 | 40.58 | 171.58 | 540 |
| 5 | first best | | 1210 | 51.64 | 5.39 | 11.45 | 68.48 | 25.17 | 156.35 | 545 |

TABLE 2. Investment and dismantling of the different technologies considered in our model, as well as total quantities invested and dismantled, total capacity change ΔCap and total $CO_2$ emissions per scenario. We abbreviate the number of candidate lines with $\ell$.

| Scenario | | | Dismantling | | | | Investment | | | | |
|---|---|---|---|---|---|---|---|---|---|---|---|
| | | | lignite | hard coal | GT | total | CCGT | CHP | total | ΔCap | $CO_2$ |
| $\ell$ | $k$ | $\beta$ | (MW) | (MW) | (MW) | (MW) | (MW) | (MW) | (MW) | (MW) | (Mt) |
| 5 | 1 | 1.00 | 506 | 0 | 479 | 986 | 0 | 7000 | 7000 | 6013 | 133.20 |
| 5 | 2 | 1.00 | 603 | 0 | 479 | 1083 | 0 | 7000 | 7000 | 5916 | 129.52 |
| 5 | 2 | 0.75 | 507 | 0 | 479 | 987 | 0 | 7000 | 7000 | 6012 | 128.54 |
| 5 | 2 | 0.50 | 3458 | 0 | 479 | 3937 | 1681 | 7000 | 8681 | 4743 | 115.89 |
| 5 | 2 | 0.25 | 3598 | 0 | 622 | 4220 | 3245 | 7000 | 10 245 | 6025 | 112.56 |
| 5 | 3 | 1.00 | 603 | 0 | 479 | 1083 | 0 | 7000 | 7000 | 5916 | 128.08 |
| 5 | 3 | 0.75 | 1277 | 0 | 479 | 1757 | 0 | 7000 | 7000 | 5242 | 124.84 |
| 5 | 3 | 0.50 | 3458 | 0 | 479 | 3937 | 1681 | 7000 | 8681 | 4743 | 114.63 |
| 5 | 3 | 0.25 | 2959 | 27 | 622 | 3608 | 3116 | 7000 | 10 116 | 6507 | 114.48 |
| 5 | 16 | 1.00 | 758 | 0 | 479 | 1237 | 0 | 7000 | 7000 | 5762 | 127.75 |
| 5 | 16 | 0.75 | 1713 | 0 | 479 | 2192 | 0 | 7000 | 7000 | 4807 | 123.16 |
| 5 | 16 | 0.50 | 3342 | 0 | 478 | 3821 | 1758 | 7000 | 8758 | 4936 | 113.88 |
| 5 | 16 | 0.25 | 4308 | 1437 | 500 | 6245 | 7587 | 7000 | 14 587 | 8342 | 104.47 |
| 15 | 1 | 1.00 | 506 | 0 | 479 | 986 | 0 | 7000 | 7000 | 6013 | 117.72 |
| 15 | 2 | 1.00 | 543 | 0 | 479 | 1023 | 0 | 7000 | 7000 | 5976 | 117.65 |
| 15 | 2 | 0.75 | 516 | 0 | 479 | 996 | 0 | 7000 | 7000 | 6003 | 117.72 |
| 15 | 2 | 0.50 | 515 | 0 | 479 | 994 | 0 | 7000 | 7000 | 6005 | 117.72 |
| 15 | 2 | 0.25 | 536 | 0 | 479 | 1016 | 0 | 7000 | 7000 | 5983 | 117.69 |
| 15 | 3 | 1.00 | 543 | 0 | 479 | 1023 | 0 | 7000 | 7000 | 5976 | 117.62 |
| 15 | 3 | 0.75 | 516 | 0 | 479 | 996 | 0 | 7000 | 7000 | 6003 | 117.73 |
| 15 | 3 | 0.50 | 524 | 0 | 479 | 1004 | 0 | 7000 | 7000 | 5995 | 117.67 |
| 15 | 16 | 1.00 | 543 | 0 | 479 | 1023 | 0 | 7000 | 7000 | 5976 | 117.67 |
| 15 | 16 | 0.75 | 1036 | 0 | 479 | 1515 | 0 | 7000 | 7000 | 5484 | 115.78 |
| 15 | 16 | 0.50 | 2369 | 0 | 479 | 2849 | 0 | 7000 | 7000 | 4150 | 111.08 |
| 15 | 16 | 0.25 | 4313 | 514 | 485 | 5313 | 4429 | 7000 | 11 429 | 6116 | 103.20 |
| 5 | first best | | 2655 | 0 | 788 | 3443 | 3620 | 7000 | 10 620 | 7176 | 113.26 |

$\beta = 0.25$. Here, a welfare gain of 1036 million € can be achieved as compared to the status quo (which is 85 % of the maximum achievable welfare gain). Implementing two zones with $\beta = 0.25$ yields a welfare gain of 1007 million € as compared to status quo (83 % of the maximum possible welfare gain). Interestingly, the introduction of 16 zones (one zone per domestic node) only leads to small marginal welfare gains in comparison with two and three zones.

For a low number of zones (two or three), welfare is higher for more restrictive inter-zonal ATCs. This is due to the fact that more restrictive inter-zonal ATCs amplify price signals during spot-market trading and ultimately lead to a more efficient allocation of generation capacity (cf. Section 4.3). Exceptions to this pattern are due to the fact that the optimal assignment of nodes to zones changes with variation of the ATCs. We will go into more detail on this point later. For the case of 16 zones, too restrictive inter-zonal ATCs can be counterproductive and lead to welfare losses as compared to scenarios with less restrictive inter-zonal ATCs. Table 2 reveals that this is due to an inefficient capacity allocation, which consists of too many gas plants at the southern nodes that are not used in the final dispatch.

4.2. **Prices.** Table 1 also indicates how these welfare gains are reflected in the electricity prices. The higher the welfare gains from optimal zoning, the lower the corrected average electricity price $p^{\text{corr}}$, as from the way we model $p^{\text{corr}}$, welfare is reflected directly in the corrected average spot market price.

In the status quo, the high corrected average price (75.12 €/MWh) is composed of a low spot-market price and considerable fees. This is due to the fact that missing congestion management at the spot market yields considerable network management cost. These costs are transferred to the consumer via network fees. In the first-best scenario, the corrected average electricity price is considerably lower (68.48 €/MWh). This is mainly due to a massive decrease in network fees.

The average price span $\Delta p^{\text{avg}}$ is typically larger for low inter-zonal ATCs. An exception occurs for the case of two zones and rather restrictive ATCs. Here, the average price spread for $\beta = 0.25$ is lower than for $\beta = 0.5$. The reason is that a change in the optimal partition of nodes (see Section 4.4) induces a change in the demand distribution between zones: For $\beta = 0.25$, demand in the northern zone is higher, while demand in the southern zone is lower as compared to $\beta = 0.5$, leading to a lower average price spread between zones for the more restrictive ATC. In general, average price differences are quite moderate, whereas they can be substantial in certain hours, as the maximum price spread across all hours, $\Delta p^{\max}$, reveals. Again, the maximum spread becomes typically larger for low inter-zonal ATCs.

Figures 3 and 4 show the price developments over time for both zones in scenario [5-2-0.25] in February and June, respectively. A large part of price differences occurs in hours with prices equal to 0 in the northern zone due to a high RES feed-in. With restrictive inter-zonal ATCs, not all of the excess electricity produced by RES can be sold to the southern zone at the spot market. Therefore, prices are higher in the southern zone in those hours. Figures 3 and 4 also demonstrate that price differences are higher in winter than in summer. In winter, high wind feed-in in the northern zone and, at the same time, more conventional electricity production in the south lead to substantial price differences. In summer, RES production is more evenly distributed, as there is less feed-in from wind plants and more feed-in from PV plants, which are more productive in the south.

4.3. **Generation Capacity Investment.** Price zones do not only affect production incentives in the short run. Due to the different profit opportunities across zones they also affect investment incentives in the long run. In the following, we first give an overview of the effects on the composition of the generation mix. Later, we also show how zonal pricing affects the location of plants.

Table 2 shows the optimal generation investment and dismantling decisions for all scenarios. In the absence of price zones we observe a moderate dismantling of lignite and gas capacity and, at the same time, an increase of CHP plants up to the limit of 7000 MW installed capacity. The introduction of price zones leads to a more pronounced switch from lignite to CHP plants in the sense that more lignite capacity, which is mainly located in the northern nodes is dismantled. For restrictive inter-zonal ATCs, i.e., $\beta \leq 0.5$, lignite capacity is moreover massively substituted by gas capacity. This is also the case in the first-best benchmark. The switch from lignite to gas has a considerable impact on $CO_2$ emissions. Emissions decrease by up to 15 % as compared to the case with a uniform price zone.

Note that the switch from lignite to gas and CHP with price zones and restrictive ATCs is due to higher peak prices in the southern zone as compared to the scenario without price zones. This induces investment incentives for gas and CHP in the south, where they can profitably operate in expectation. Obviously, beyond the effect on the generation mix, we should expect an effect on the location of plants, which we discuss in the following section.

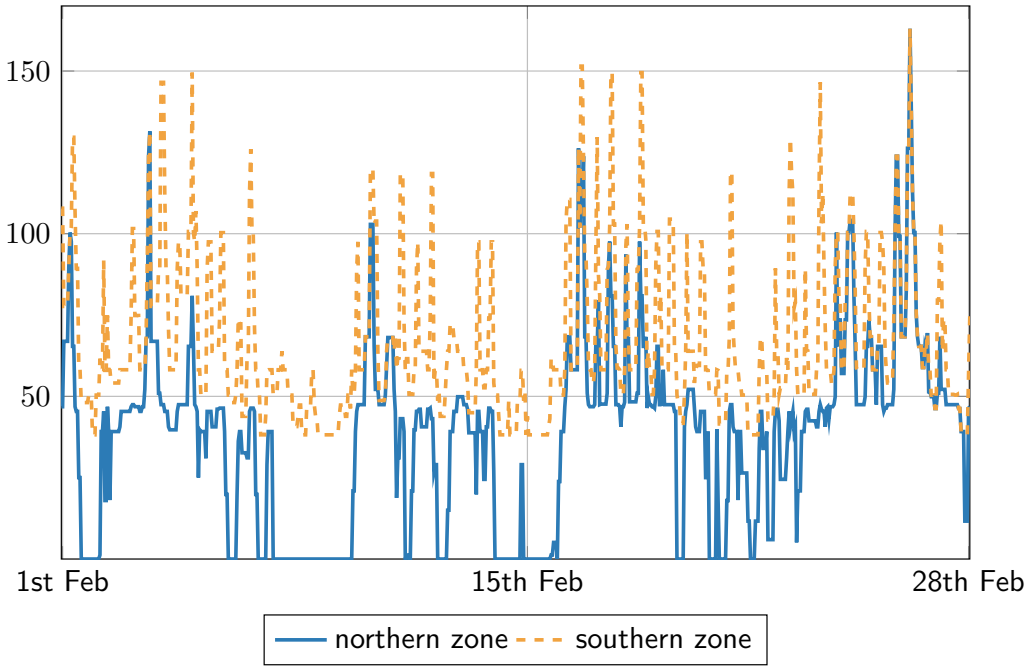


FIGURE 3. Hourly zonal prices (in €/MWh) in February for scenario [5-2-0.25]. The solid line represents prices in the northern zone, the dashed line prices in the southern zone.

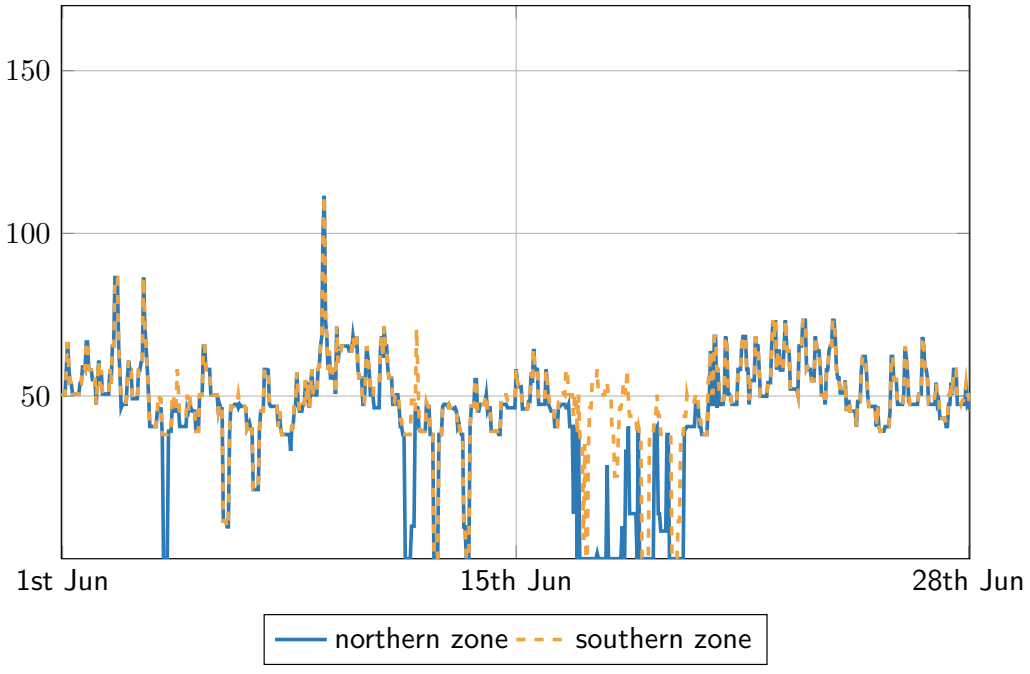


FIGURE 4. Hourly zonal prices (in €/MWh) in June for scenario [5-2-0.25]. The solid line represents prices in the northern zone, the dashed line prices in the southern zone.

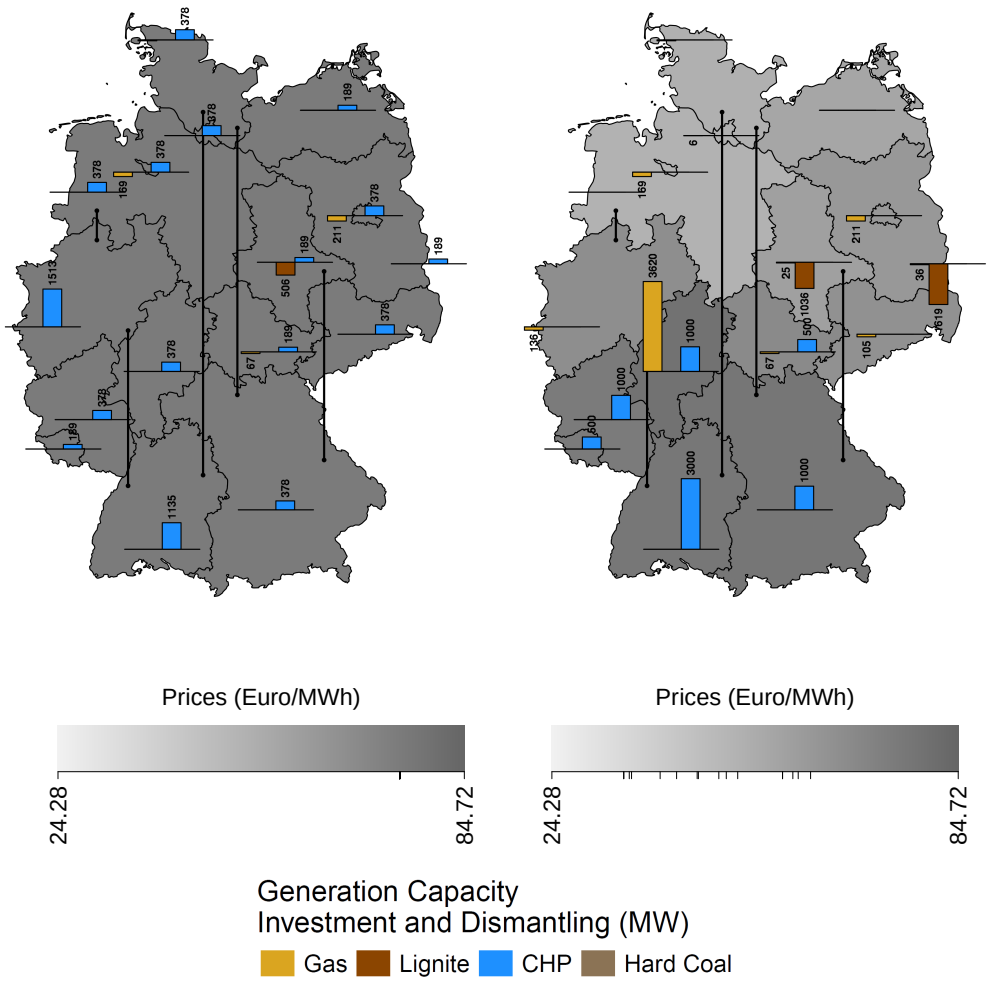


FIGURE 5. Generation investment and dismantling and prices for status quo (left) and first best (right). Darker shades of gray indicate higher prices, ticks on the colorbar indicate prices of each zone.

4.4. **Optimal Zoning.** In this section we present detailed results on the optimal zoning and the corresponding equilibrium allocation of conventional generation capacity.

Figure 5 illustrates our two benchmark scenarios. On the left, we display results in the status-quo scenario with a single price zone. On the right, we present the first-best scenario. The figures show investment and dismantling of generation capacity (for lignite, hard coal, gas, and CHP), line expansion, and price levels (shades of gray of the different regions). We clearly observe the moderate dismantling of lignite and expansion of CHP capacity in the status quo scenario. Due to same spot-market price for all regions, CHP expansion takes place throughout the country. In the first-best scenario, high RES production combined with low regional demand in the north leads to relatively low prices in the north and higher prices in southern regions. This induces differentiated and also more pronounced incentives to invest and dismantle. The more pronounced switch from lignite to gas and CHP already pointed to in the previous section goes along with a clear adjustment of locational decisions.

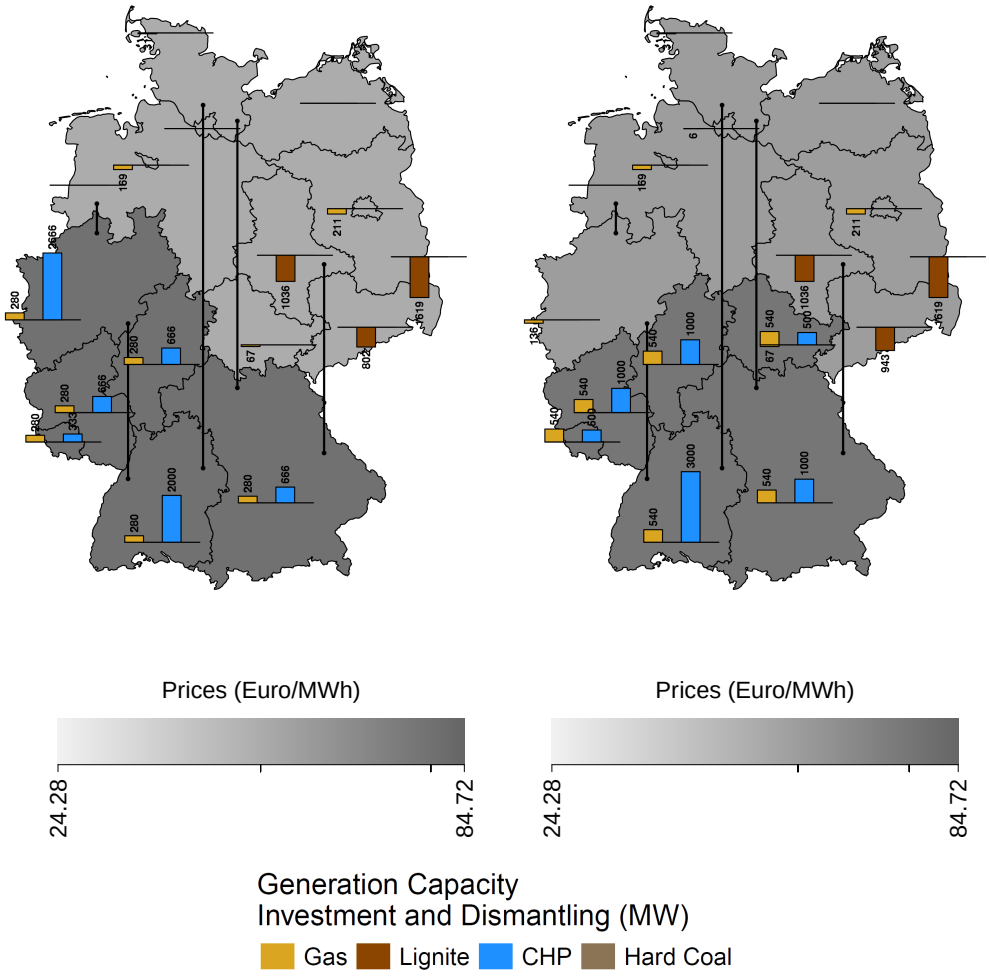


FIGURE 6. Generation investment and dismantling and optimal zoning for scenario [5-2-0.5] (left) and [5-2-0.25] (right). Darker shades of gray indicate higher prices, ticks on the colorbar indicate prices for each zone.

Obviously, dismantling of lignite plants takes place in the north-east, while expansion of gas and CHP capacity is observed in the south.

Figure 6 shows the optimal zonal configuration for 2 zones with two different ATCs, $\beta = 0.5$ (left) and $\beta = 0.25$ (right). For both scenarios, partitioning into a northern and southern zone is optimal. Due to the location of load centers and RES generation, prices in the northern zone are significantly lower than prices in the southern zone.

The figure particularly highlights the crucial importance of inter-zonal ATCs for determining the welfare-maximal zonal configuration. For restrictive inter-zonal ATCs (right figure), North Rhine Westphalia (NRW) is assigned to the northern zone. This makes it possible to meet the high industrial demand in NRW with (renewable) energy from the north at the spot market. For larger inter-zonal ATCs (left figure), NRW is assigned to the southern zone and demand is met by renewable energy traded at the spot market as well as a significant CHP capacity that is installed. Obviously, ATCs crucially affect the optimal zoning and the associated allocation of capacities.

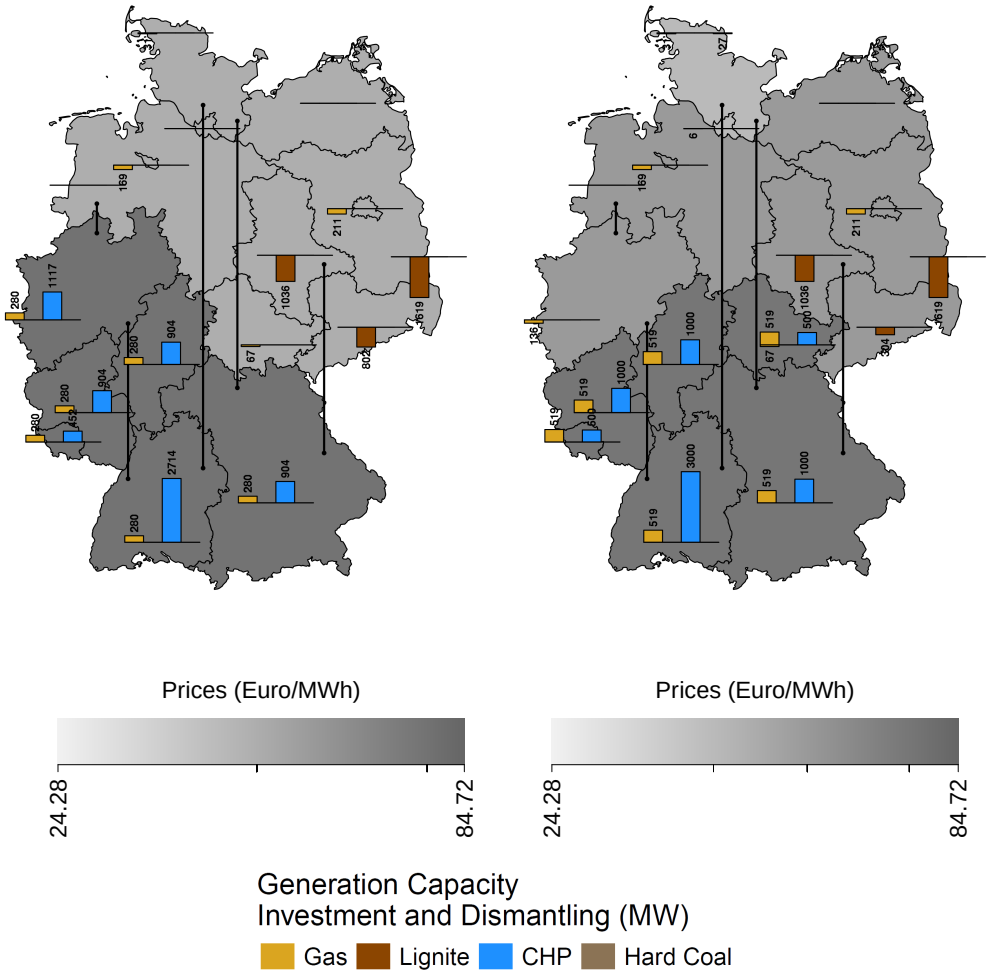


FIGURE 7. Generation investment and dismantling and optimal zoning for scenario [5-3-0.5] (left) and [5-3-0.25] (right). Darker shades of gray indicate higher prices, ticks on the colorbar indicate prices for each zone.

Figure 7 presents the optimal zonal configuration for three zones, again with two different ATCs, $\beta = 0.5$ (left) and $\beta = 0.25$ (right). For moderate inter-zonal ATCs, de facto only two zones with different prices are distinguishable. Only for $\beta = 0.25$, a third region with a separate electricity price emerges, which includes the nodes of Schleswig-Holstein and Hamburg. Note that this optimal zoning is in contrast to what would result from clustering regions with similar prices from the first-best scenario (cf. Figure 5). The latter would rather lead to a northern price zone including Lower Saxony. Nodal (first best) prices thus do not seem to be a good indicator for the optimal zonal configuration for a limited number of zones.

4.5. **Congestion Management and Network Costs.** Table 3 shows all costs and revenues that the TSO faces. Redispatch costs potentially occur from redispatching generators ($G$) and/or consumers ($C$). Network costs are composed of network investment cost $E^{\text{inv}}$ minus revenues from inter-zonal trade $-R^{\text{dom}}$ and $-R^{\text{abr}}$. Note that since the table displays costs, network revenues come as negative numbers.

TABLE 3. Congestion management costs (million €). Redispatch costs consist of costs to redispatch generators ($G$) and consumers ($C$). Network costs are composed of domestic and abroad network revenues, $R^{\text{dom}}$ and $R^{\text{abr}}$, and total line investment costs $E^{\text{inv}}$. For all scenarios, there are additional maintenance costs of 3000 million €. We abbreviate the number of candidate lines with $\ell$.

| Scenario | | | Redispatch Costs | | Network Costs | | | |
|---|---|---|---|---|---|---|---|---|
| $\ell$ | $k$ | $\beta$ | $G$ | $C$ | $R^{\text{dom}}$ | $R^{\text{abr}}$ | $E^{\text{inv}}$ | total |
| 5 | 1 | 1.00 | 1593 | 676 | 0 | −190 | 489 | 5569 |
| 5 | 2 | 1.00 | 1332 | 360 | −114 | −187 | 489 | 4880 |
| 5 | 2 | 0.75 | 1273 | 279 | 0 | −190 | 489 | 4851 |
| 5 | 2 | 0.50 | 45 | 53 | −441 | −172 | 489 | 2973 |
| 5 | 2 | 0.25 | 560 | 6 | −196 | −178 | 489 | 3681 |
| 5 | 3 | 1.00 | 1213 | 288 | −114 | −187 | 489 | 4689 |
| 5 | 3 | 0.75 | 824 | 219 | −296 | −180 | 489 | 4055 |
| 5 | 3 | 0.50 | −93 | 24 | −441 | −172 | 489 | 2805 |
| 5 | 3 | 0.25 | 420 | 2 | −239 | −177 | 489 | 3495 |
| 5 | 16 | 1.00 | 1225 | 298 | −121 | −187 | 489 | 4705 |
| 5 | 16 | 0.75 | 791 | 226 | −324 | −180 | 489 | 4001 |
| 5 | 16 | 0.50 | −325 | 11 | −504 | −172 | 489 | 2498 |
| 5 | 16 | 0.25 | −2314 | 0 | −418 | −168 | 489 | 587 |
| 15 | 1 | 1.00 | 20 | 0 | 0 | −190 | 3249 | 6079 |
| 15 | 2 | 1.00 | 11 | 0 | −7 | −190 | 3249 | 6063 |
| 15 | 2 | 0.75 | 5 | 0 | −29 | −189 | 3249 | 6035 |
| 15 | 2 | 0.50 | 12 | 0 | −4 | −190 | 3249 | 6066 |
| 15 | 2 | 0.25 | 10 | 0 | −7 | −190 | 3249 | 6062 |
| 15 | 3 | 1.00 | 10 | 0 | −7 | −190 | 3249 | 6063 |
| 15 | 3 | 0.75 | 5 | 0 | −29 | −189 | 3249 | 6035 |
| 15 | 3 | 0.50 | 5 | 0 | −21 | −189 | 3249 | 6043 |
| 15 | 16 | 1.00 | 11 | 0 | −7 | −190 | 3249 | 6063 |
| 15 | 16 | 0.75 | −18 | 0 | −55 | −187 | 3249 | 5987 |
| 15 | 16 | 0.50 | −307 | 0 | −310 | −179 | 3249 | 5450 |
| 15 | 16 | 0.25 | −1906 | 0 | −499 | −169 | 3249 | 3673 |
| 5 | first best | | — | — | −372 | −178 | 489 | 2938 |

Among the scenarios where the network is expanded by five transmission lines, the status quo is the scenario with the highest expenses for congestion management. This is intuitive, as network restrictions are completely neglected during spot-market trading. On the contrary, in the first-best scenario the TSO's costs are determined by network expansion costs only, as network restrictions are fully taken into account during spot-market trading.

The introduction of optimal price zones ensures that transmission constraints are at least partially taken into account upon spot-market trading and thus leads to a reduction in redispatch costs.

Although the number of zones is important, the size of inter-zonal ATCs also plays a major role for redispatch costs. We observe that redispatch costs are generally lower for more restrictive inter-zonal ATCs. The reason is that generation capacity investment

TABLE 4. RES curtailment during spot-market trading and after redispatch. The potential RES generation is 277 TWh in all scenarios. We abbreviate the number of candidate lines with $\ell$.

| Scenario | | | Load Shedding | RES Spot | | | RES Final | | |
|---|---|---|---|---|---|---|---|---|---|
| | | | | feed-in | curt. | curt. ratio | feed-in | curt. | curt. ratio |
| $\ell$ | $k$ | $\beta$ | (TWh) | (TWh) | (TWh) | (%) | (TWh) | (TWh) | (%) |
| 5 | 1 | 1.00 | 6 | 272 | 4 | 1.70 | 241 | 36 | 13.10 |
| 5 | 2 | 1.00 | 3 | 271 | 6 | 2.30 | 244 | 32 | 11.80 |
| 5 | 2 | 0.75 | 2 | 272 | 4 | 1.70 | 247 | 29 | 10.80 |
| 5 | 2 | 0.50 | 0 | 249 | 28 | 10.20 | 251 | 26 | 9.40 |
| 5 | 2 | 0.25 | 0 | 266 | 11 | 4.00 | 255 | 21 | 7.90 |
| 5 | 3 | 1.00 | 2 | 271 | 6 | 2.30 | 247 | 30 | 10.90 |
| 5 | 3 | 0.75 | 1 | 264 | 13 | 4.80 | 249 | 28 | 10.20 |
| 5 | 3 | 0.50 | 0 | 249 | 28 | 10.20 | 253 | 23 | 8.60 |
| 5 | 3 | 0.25 | 0 | 264 | 13 | 4.80 | 255 | 21 | 7.70 |
| 5 | 16 | 1.00 | 2 | 271 | 6 | 2.30 | 246 | 30 | 11.00 |
| 5 | 16 | 0.75 | 1 | 263 | 13 | 4.90 | 249 | 28 | 10.10 |
| 5 | 16 | 0.50 | 0 | 245 | 32 | 11.60 | 254 | 23 | 8.40 |
| 5 | 16 | 0.25 | 0 | 211 | 66 | 23.80 | 257 | 19 | 7.10 |
| 5 | first best | | — | — | — | — | 258 | 19 | 6.90 |

and spot-market trading are more efficient as scarcities are partly reflected by electricity prices. For scenarios with very restrictive inter-zonal ATCs, redispatch costs even become negative. This shows that too restrictive inter-zonal ATCs lead to oversteering in capacity investment and spot-market trading. More precisely, there is too little capacity for inter-zonal trade during spot-market trading, which leads to suboptimal welfare results. During redispatch, this missing trading volume is compensated, resulting in welfare gains. Note that scenarios [5-2-0.25] and [5-3-0.25] have higher redispatch costs than those with less restrictive inter-zonal ATCs. This is due to the fact that the resulting optimal zonal configuration is different in these scenarios. As NRW is assigned to the northern zone for very restrictive inter-zonal ATCs, no grid restrictions between nodes with high RES generation and NRW are taken into account during spot-market trading. This leads to higher costs in the subsequent redispatch to compensate for network bottlenecks.

We now consider scenarios where the network is expanded by all 15 transmission lines. It becomes obvious from Table 3 that redispatch costs only play a minor role in scenarios with two or three price zones. In the case of 16 price zones, restricting inter-zonal ATCs very quickly leads to negative redispatch costs, which again means an oversteering during spot-market trading, which is offset by redispatch.

In most scenarios, overall welfare gains from market splitting are lower than the reduction in congestion management cost as compared to status quo. The reason is that electricity production is in general more expensive in those scenarios with price zones and restrictive inter-zonal ATCs, as hard coal and lignite plants with lower variable costs are dismantled in the north, whereas more expensive gas plants are built in the south.

4.6. **Renewables.** In order to provide an intuition of how transmission constraints affect renewable production, in Table 4 we present details on load shedding and RES curtailment during spot-market trading as well as on the final RES quantities after redispatch. Since RES capacities and hourly weather data are given exogenously, RES potential is the same in all scenarios (277 TWh).

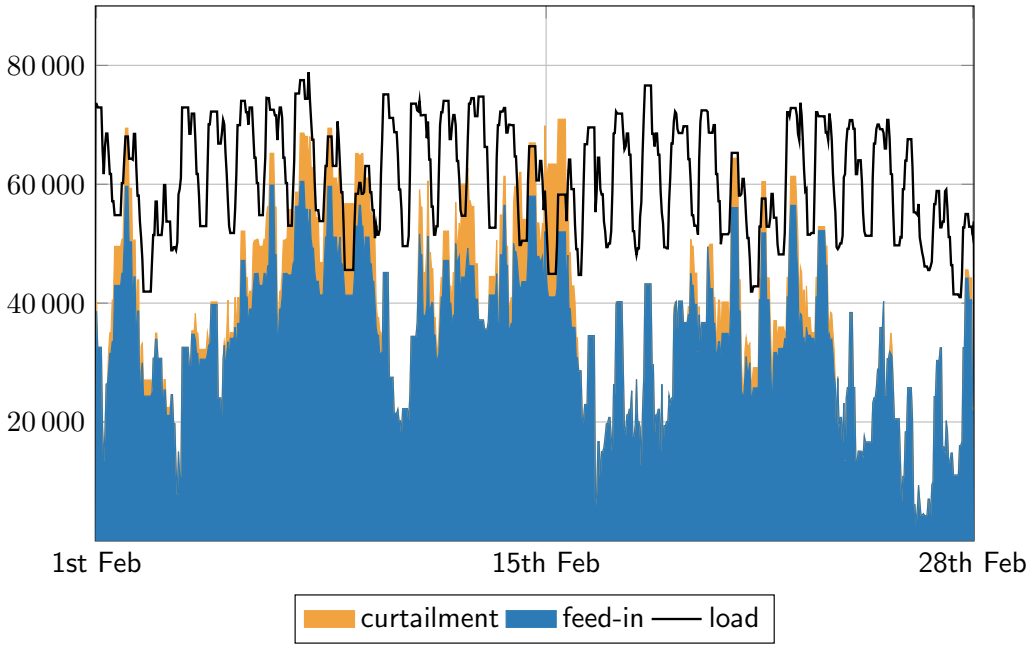


FIGURE 8. Hourly renewables feed-in and curtailment (in MWh) in February for the scenario [5-2-0.25].

The final amount of curtailment is highest in the status-quo scenario. Here, regional price signals are missing, hence consumption does not react sufficiently to changes in supply. The more zones are introduced, the more accurate variations in generation quantities are reflected by prices, which leads to a more effective reaction of consumption and thus less curtailment. This effect is reinforced by restrictive inter-zonal ATCs, which intensify price signals during spot-market trading. Consequently, less RES curtailment is necessary when price zones with restrictive inter-zonal ATCs are implemented.

In scenarios where the network is expanded by 15 lines, only minor amounts of RES are curtailed, as there is enough transmission capacity to distribute RES capacity to load centers. Hence, zonal configuration and inter-zonal ATCs hardly have any effect. Therefore, we omit the results in Table 4.

In practice, RES curtailment is proposed in the form of peak shaving in hours with high RES generation. This is, however, suboptimal as it does not take into account the current level of load. In our computations, we assume efficient curtailment, i.e., we assume that RES are only curtailed in case of excess supply that cannot be transported to load centers via the current network. Curtailment takes place at the spot market (in order to avoid prices below zero), as well as upon redispatch. Figure 8 and Figure 9 provide information on the pattern of curtailment in a typical winter and summer month, respectively. In summer, renewable production is moderate and determined by solar peaks at daytime. Curtailment occurs rarely and if so then due to excess supply; cf. Figure 9. In winter, RES feed-in is mostly driven by wind turbines at a higher level. Here, curtailment of peaks is frequent. Excess supply, moreover, is not the main reason for curtailment. Instead, transmission constraints often require curtailment due to disparate locations of wind supply (north) and load centers (south); see Figure 8.

## 5. CONCLUSION

In this paper, we consider electricity market designs with a zonal pricing regime, as today established, e.g., in Europe or Australia. We present an approach to determine the

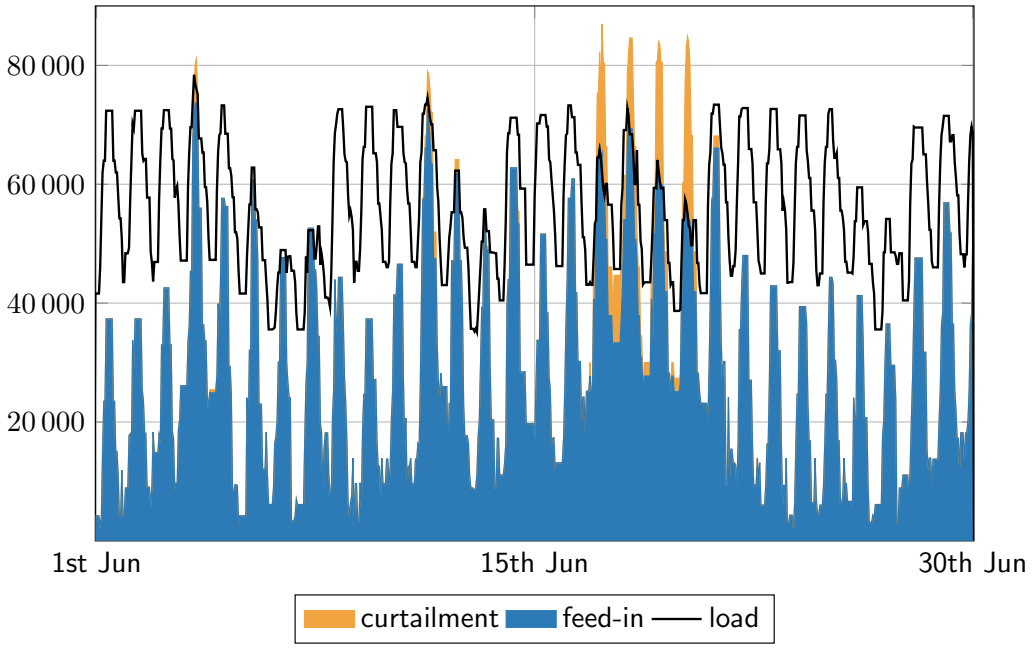


FIGURE 9. Hourly renewables feed-in and curtailment (in MWh) in June for the scenario [5-2-0.25].

optimal zonal configuration for a predetermined number of zones and available transfer capacities between zones. In doing so, we particularly focus on the long-run perspective. In addition to short-run effects of regionally differentiated spot-market prices, we explicitly capture the effects of zonal pricing on incentives to invest in generation capacity.

Our modeling extends previous contributions on multilevel electricity market models (Grimm et al. 2019, 2016a; Kleinert and Schmidt 2019) that capture the interdependencies of the regulator's decision on the zonal configuration and the firms' decisions on investment in generation capacity and electricity production. Further, we apply the problem-tailored generalized Benders decomposition approach that has been developed in Grimm et al. (2019) and Kleinert and Schmidt (2019), and extend it to cope with our specific setup.

We illustrate the capability of the approach by applying it to a model of the German market area. We derive a simplified representation of the German electricity market from data of the scenario framework of the German network development plan. To adequately assess investment incentives for different generation technologies and, at the same time, solve realistic instances, we also simplify the time series of electricity demand parameters for our numerical application such that the incentive effect of price peaks is not distorted. In particular, we combine density-based and $k$-means clustering techniques for constructing smaller scenario sets that yield computationally more tractable instances.

The analysis yields various insights. First, a considerable share of the maximum possible welfare gains can already be achieved by implementing few (two or three) optimally configured price zones with restrictive inter-zonal ATCs. Second, ATCs between zones are an important influencing factor for the achievable welfare gains and investment incentives. In particular, they are a key determinant of the assignment of nodes to zones and the price differences. Third, adjusted investment and production incentives with two or three price zones imply a substitution of coal-fired plants by gas-fired and CHP plants associated with a considerable drop in $CO_2$ emissions. Finally, hypothetical nodal prices are not a good guidance to partition nodes into optimal zones. Overall, the analysis reveals that optimal zoning depends on a large variety of parameters and probably changes over time. Thus,

the regulator faces an extremely complex problem, that can be tackled using the models and techniques presented in Grimm et al. (2019), Kleinert and Schmidt (2019) and in this paper.

## Acknowledgements

This research has been performed as part of the Energie Campus Nürnberg (EnCN) and is supported by funding of the Bavarian State Government and the Emerging Field Initiative (EFI) of the Friedrich-Alexander-Universität Erlangen-Nürnberg through the project "Sustainable Business Models in Energy Markets". The authors thank the Deutsche Forschungsgemeinschaft for their support within project A05, B06, B08, and B09 in the Sonderforschungsbereich / Transregio 154 Mathematical Modelling, Simulation and Optimization using the Example of Gas Networks. This paper has received funding from the European Union's Horizon 2020 research and innovation programme under the Marie Skłodowska-Curie grant agreement No 764759.

## References

50Hertz (2015). *Netzbelastung in der Regelzone*. URL: http://www.50hertz.com/de/Kennzahlen/Netzbelastung.

AgoraEnergiewende (2015). *Current and Future Cost of Photovoltaics*. URL: https://www.ise.fraunhofer.de/content/dam/ise/de/documents/publications/studies/AgoraEnergiewende_Current_and_Future_Cost_of_PV_Feb2015_web.pdf.

Amprion (2015). *Das 380/220 kV-Netz der Amprion GmbH*. URL: https://web.archive.org/web/20150417190917/https://www.amprion.net/das-380-220-kv-netz.

Arrow, K. J. and G. Debreu (1954). "Existence of an equilibrium for a competitive economy." In: *Econometrica: Journal of the Econometric Society* 22.3, pp. 265–290. DOI: 10.2307/1907353.

Arthur, D. and S. Vassilvitskii (2007). "$k$-means++: The advantages of careful seeding." In: *Proceedings of the eighteenth annual ACM-SIAM symposium on Discrete algorithms*. Society for Industrial and Applied Mathematics, pp. 1027–1035.

BDEW (2015). *Erneuerbare Energien und das EEG: Zahlen, Fakten, Grafiken (2015)*. Tech. rep.

Bertsch, J., S. Hagspiel, and L. Just (2016). "Congestion management in power systems." In: *Journal of Regulatory Economics* 50.3, pp. 290–327. DOI: 10.1007/s11149-016-9310-x.

BGBl (2005). *Verordnung über die Entgelte für den Zugang zu Elektrizitätsversorgungsnetzen (Stromnetzentgeltverordnung - StromNEV)*. Anlage 1 (zu § 6 Abs. 5 Satz 1) Betriebsgewöhnliche Nutzungsdauern. URL: https://www.gesetze-im-internet.de/stromnev/anlage_1.html.

Bjørndal, M. and K. Jørnsten (2001). "Zonal pricing in a deregulated electricity market." In: *The Energy Journal*, pp. 51–73. DOI: 10.5547/ISSN0195-6574-EJ-Vol22-No1-3.

BMVI (2015). *Räumlich differenzierte Flächen-Potenziale für erneuerbare Energien in Deutschland*. URL: https://www.bbr.bund.de/BBSR/DE/Veroeffentlichungen/ministerien/BMVI/BMVIOnline/2015/DL_BMVI_Online_08_15.pdf?__blob=publicationFile&v=2.

BNetzA (2015). *EEG in Zahlen 2014*. URL: https://www.bundesnetzagentur.de/SharedDocs/Downloads/DE/Sachgebiete/Energie/Unternehmen_Institutionen/ErneuerbareEnergien/ZahlenDatenInformationen/EEGinZahlen_2014_BF.pdf?__blob=publicationFile&v=4.

– (2016a). *Genehmigung des Szenariorahmens für die Netzentwicklungspläne Strom 2017-2030*. URL: https://data.netzausbau.de/2030/Szenariorahmen_2030_Genehmigung.pdf.

– (2016b). *Kraftwerksliste zu der Genehmigung des Szenariorahmens für die Netzentwicklungspläne Strom 2017-2030*. URL: https://www.netzentwicklungsplan.de/sites/default/files/paragraphs-files/20190630_kraftwerksliste_bnetza_2030_0.pdf.

Boucher, J. and Y. Smeers (2001). "Alternative Models of Restructured Electricity Systems, Part 1: No Market Power." In: *Operations Research* 49.6, pp. 821–838. DOI: 10.1287/opre.49.6.821.10017.

Breuer, C. and A. Moser (2014). "Optimized bidding area delimitations and their impact on electricity markets and congestion management." In: *11th International Conference on the European Energy Market (EEM14)*, pp. 1–5. DOI: 10.1109/EEM.2014.6861218.

Burstedde, B. (2012). "From nodal to zonal pricing: A bottom-up approach to the second-best." In: *9th International Conference on the European Energy Market, EEM 12*, pp. 1–8. DOI: 10.1109/EEM.2012.6254665.

BWE (2012). *Potenzial der Windenergienutzung an Land*. URL: https://www.wind-energie.de/fileadmin/redaktion/dokumente/publikationen-oeffentlich/themen/01-mensch-und-umwelt/03-naturschutz/bwe_potenzialstudie_kurzfassung_2012-03.pdf.

Daxhelet, O. and Y. Smeers (2007). "The EU regulation on cross-border trade of electricity: A two-stage equilibrium model." In: *European Journal of Operational Research* 181.3, pp. 1396–1412. DOI: 10.1016/j.ejor.2005.12.040.

Dempe, S., V. Kalashnikov, G. A. Pérez-Valdés, and N. Kalashnykova (2015). "Bilevel Programming Problems." In: *Energy Systems. Springer, Berlin*.

Destatis (2015). *Bodenfläche nach Art der tatsächlichen Nutzung*. Tech. rep. Wiesbaden. URL: https://www.destatis.de/DE/Publikationen/Thematisch/LandForstwirtschaft/Flaechennutzung/Bodenflaechennutzung2030510147004.pdf?__blob=publicationFile.

– (2016a). *Elektrizitätserzeugung, Nettowärmeerzeugung, Brennstoffeinsatz: Deutschland, Monate, Energieträger*. Tech. rep. URL: https://www.govdata.de/suchen/-/details/destatis-service-43311-0002.

– (2016b). *Tabelle 43311-0002- Elektrizitätserzeugung, Nettowärmeerzeugung, Brennstoffeinsatz: Deutschland, Monate, Energieträger*. URL: https://www-genesis.destatis.de/genesis/online?sequenz=tabelleDownload&selectionname=43311-0002&regionalschluessel=&format=xlsx.

Ding, F. and J. D. Fuller (2005). "Nodal, uniform, or zonal pricing: distribution of economic surplus." In: *IEEE Transactions on Power Systems* 20.2, pp. 875–882. DOI: 10.1109/TPWRS.2005.846042.

Egerer, J., C. Gerbaulet, R. Ihlenburg, F. Kunz, B. Reinhard, C. von Hirschhausen, A. Weber, and J. Weibezahn (2014). *Electricity sector data for policy-relevant modeling: Data documentation and applications to the german and european electricity markets*. Tech. rep. Data Documentation, DIW. URL: https://www.diw.de/documents/publikationen/73/diw_01.c.440963.de/diw_datadoc_2014-072.pdf.

Egerer, J., V. Grimm, T. Kleinert, M. Schmidt, and G. Zöttl (Dec. 2019). *The Impact of Neighboring Markets on Renewable Locations, Transmission Expansion, and Generation Investment*. Tech. rep. DOI: 10.2139/ssrn.3498339.

Egerer, J., J. Weibezahn, and H. Hermann (2016). "Two price zones for the German electricity market — Market implications and distributional effects." In: *Energy Economics* 59, pp. 365–381. DOI: 10.1016/j.eneco.2016.08.002.

EnCN/FAU/Prognos (2016). *Dezentralität und Zellulare Optimierung – Auswirkungen auf den Netzausbaubedarf*. Gutachten im Auftrag der N-Ergie AG, Nürnberg. URL: https://www.fau.de/files/2016/10/Energiestudie_Studie.pdf.

ENTSO-E (2015). *All TSOs' draft proposal for Capacity Calculation Regions (CCRs)*. URL: https://consultations.entsoe.eu/system-operations/capacity-calculation-

regions/supporting_documents/All%20TSOs%20proposal%20for%20CCRs_ENTSOE%20format_v0public%20consultation_final.pdf.

ENTSO-E (2018). *First Edition of the Bidding Zone Review – Final Report*. URL: https://docstore.entsoe.eu/Documents/News/bz-review/2018-03_First_Edition_of_the_Bidding_Zone_Review.pdf.

– (2019). *Annex 1: Considerations on Bidding Zone Review Region "Central Western Europe" Bidding Zone Configurations*. URL: https://www.entsoe.eu/news/2019/10/07/bidding-zone-review-methodology-assumptions-and-configurations-submitted-to-nras/.

EnWG (2005). *Gesetz über die Elektrizitäts- und Gasversorgung (Energiewirtschaftsgesetz - EnWG)*. Energiewirtschaftsgesetz from 7. July 2005 (BGBl. I S. 1970, 3621), which was last modified through article 6 paragraph 36 on 13. April 2017 (BGBl. I p. 872).

Ester, M., H.-P. Kriegel, J. Sander, X. Xu, et al. (1996). "A density-based algorithm for discovering clusters in large spatial databases with noise." In: *Proceedings of the Second International Conference on Knowledge Discovery and Data Mining*. KDD'96. Portland, Oregon: AAAI Press, pp. 226–231. URL: http://dl.acm.org/citation.cfm?id=3001460.3001507.

European Commission (2015). *Commmission Regulation (EU) 2015/1222 of 24 July 2015 establishing a guideline on capacity allocation and congestion management*. URL: https://eur-lex.europa.eu/legal-content/EN/TXT/PDF/?uri=CELEX:32015R1222&%09%09%09from=EN.

Felling, T. and C. Weber (2017). *Consistent and Robust Delimitation of Price Zones Under Uncertainty with an Application to Central Western Europe*. HEMF Working Paper No.06/2017. University of Duisburg-Essen. DOI: 10.2139/ssrn.2996385.

Feng, Y. and S. M. Ryan (2013). "Scenario construction and reduction applied to stochastic power generation expansion planning." In: *Computers & Operations Research* 40.1, pp. 9–23. DOI: 10.1016/j.cor.2012.05.005.

Fischetti, M., I. Ljubić, M. Monaci, and M. Sinnl (2017). "A New General-Purpose Algorithm for Mixed-Integer Bilevel Linear Programs." In: *Operations Research* 65.6, pp. 1615–1637. DOI: 10.1287/opre.2017.1650.

Fürsch, M., S. Hagspiel, C. Jägemann, S. Nagl, D. Lindenberger, and E. Tröster (2013). "The role of grid extensions in a cost-efficient transformation of the European electricity system until 2050." In: *Applied Energy* 104, pp. 642–652.

Gerbaulet, C., J. Egerer, P. Oei, J. Paeper, and C. von Hirschhausen (2012). "Die Zukunft der Braunkohle in Deutschland im Rahmen der Energiewende." In: *DIW Politikberatung kompakt* 69. URL: https://www.diw.de/documents/publikationen/73/diw_01.c.412261.de/diwkompakt_2012-069.pdf.

Gerbaulet, C. and C. Lorenz (2017). *dynELMOD: A dynamic investment and dispatch model for the future european electricity market*. Tech. rep. DIW Data Documentation.

German TSOs (2014a). *Netzentwicklungsplan Strom 2014, Zweiter Entwurf der Übertragungsnetzbetreiber*. Tech. rep.

– (2014b). *Szenariorahmen für die Netzentwicklungspläne Strom 2015, Entwurf der Übertragungsnetzbetreiber*. Tech. rep.

– (2016). *Szenariorahmen für die Netzentwicklungspläne Strom 2030, Entwurf der Übertragungsnetzbetreiber*. Tech. rep.

– (2017). *Netzentwicklungsplan Strom 2030, Version 2017, Erster Entwurf der Übertragungsnetzbetreiber*. Tech. rep.

Grimm, V., T. Kleinert, F. Liers, M. Schmidt, and G. Zöttl (2019). "Optimal price zones of electricity markets: a mixed-integer multilevel model and global solution approaches." In: *Optimization Methods and Software* 34.2, pp. 406–436. DOI: 10.1080/10556788.2017.1401069.

Grimm, V., A. Martin, M. Schmidt, M. Weibelzahl, and G. Zöttl (2016a). "Transmission and Generation Investment in Electricity Markets: The Effects of Market Splitting and Network Fee Regimes." In: *European Journal of Operational Research* 254.2, pp. 493–509. DOI: 10.1016/j.ejor.2016.03.044.

Grimm, V., A. Martin, M. Weibelzahl, and G. Zöttl (2016b). "On the long run effects of market splitting: Why more price zones might decrease welfare." In: *Energy Policy* 94, pp. 453–467. DOI: 10.1016/j.enpol.2015.11.010.

Grimm, V., L. Schewe, M. Schmidt, and G. Zöttl (2017). "Uniqueness of market equilibrium on a network: A peak-load pricing approach." In: *European Journal of Operational Research* 261.3, pp. 971–983. DOI: 10.1016/j.ejor.2017.03.036.

Grimm, V. and G. Zöttl (2013). "Investment incentives and electricity spot market competition." In: *Journal of Economics & Management Strategy* 22.4, pp. 832–851. DOI: 10.1111/jems.12029.

Hojny, C., I. Joormann, H. Lüthen, and M. Schmidt (2018). *Mixed-Integer Programming Techniques for the Connected Max-k-Cut Problem.* Tech. rep. URL: http://www.optimization-online.org/DB_HTML/2018/07/6738.html.

Holmberg, P. and E. Lazarczyk (2015). "Comparison of congestion management techniques: Nodal, zonal and discriminatory pricing." In: *Energy Journal* 36.2, pp. 145–166. DOI: 10.5547/01956574.36.2.7.

Hu, X. and D. Ralph (2007). "Using EPECs to model bilevel games in restructured electricity markets with locational prices." In: *Operations Research* 55.5, pp. 809–827. DOI: 10.1287/opre.1070.0431.

Huppmann, D. and J. Egerer (2015). "National-strategic investment in European power transmission capacity." In: *European Journal of Operational Research* 247.1, pp. 191–203. DOI: http://dx.doi.org/10.1016/j.ejor.2015.05.056. URL: http://www.sciencedirect.com/science/article/pii/S0377221715004671.

IWES (2012). *Energiewirtschaftliche Bedeutung der Offshore-Windindustrie für die Energiewende.* URL: http://www.fraunhofer.de/content/dam/zv/de/forschungsthemen/energie/Energiewirtschaftliche-Bedeutung-von-Offshore-Windenergie.pdf.

Jensen, T. V., J. Kazempour, and P. Pinson (2017). "Cost-Optimal ATCs in Zonal Electricity Markets." In: *IEEE Transactions on Power Systems* 33.4, pp. 3624–3633. DOI: 10.1109/TPWRS.2017.2786940.

Joost (2015). *Powerland - Hochspannungsleitungen in Deutschland.* URL: https://web.archive.org/web/20160109230306/http://powerland.bplaced.net:80/osm-power.htm.

Kemfert, C., F. Kunz, and J. Rosellón (2016). "A welfare analysis of electricity transmission planning in Germany." In: *Energy Policy* 94, pp. 446–452.

Kießling, F., P. Nefzger, and U. Kaintzyk (2001). *Freileitungen: Planung, Berechnung, Ausführung.* Berlin Heidelberg: Springer-Verlag.

Kleinert, T. and M. Schmidt (2019). "Global Optimization of Multilevel Electricity Market Models Including Network Design and Graph Partitioning." In: *Discrete Optimization* 33, pp. 43–69. DOI: 10.1016/j.disopt.2019.02.002.

Konstantin, P. (2013). *Praxisbuch Energiewirtschaft.* Berlin-Heidelberg: Springer-Verlag.

Krebs, V., L. Schewe, and M. Schmidt (2018). "Uniqueness and Multiplicity of Market Equilibria on DC Power Flow Networks." In: *European Journal of Operational Research* 271.1, pp. 165–178. DOI: 10.1016/j.ejor.2018.05.016.

Krebs, V. and M. Schmidt (2018). "Uniqueness of market equilibria on networks with transport costs." In: *Operations Research Perspectives* 5, pp. 169–173. DOI: 10.1016/j.orp.2018.05.002.

Lara, C. L., D. S. Mallapragada, D. J. Papageorgiou, A. Venkatesh, and I. E. Grossmann (2018). "Deterministic electric power infrastructure planning: Mixed-integer programming model and nested decomposition algorithm." In: *European Journal of Operational Research* 271.3, pp. 1037–1054. DOI: 10.1016/j.ejor.2018.05.039.

Leuthold, F., H. Weigt, and C. Von Hirschhausen (2008). "Efficient pricing for European electricity networks–The theory of nodal pricing applied to feeding-in wind in Germany." In: *Utilities Policy* 16.4, pp. 284–291.

Lodi, A., T. K. Ralphs, and G. J. Woeginger (2014). "Bilevel programming and the separation problem." In: *Mathematical Programming* 146.1-2, pp. 437–458. DOI: 10.1007/s10107-013-0700-x.

Moore, J. T. and J. F. Bard (1990). "The mixed integer linear bilevel programming problem." In: *Operations Research* 38.5, pp. 911–921. DOI: 10.1287/opre.38.5.911.

Murphy, F. H. and Y. Smeers (2005). "Generation capacity expansion in imperfectly competitive restructured electricity markets." In: *Operations Research* 53.4, pp. 646–661. DOI: 10.1287/opre.1050.0211.

Neuhoff, K., J. Barquin, J. W. Bialek, R. Boyd, C. J. Dent, F. Echavarren, T. Grau, C. von Hirschhausen, B. F. Hobbs, F. Kunz, C. Nabe, G. Papaefthymiou, C. Weber, and H. Weigt (2013). "Renewable electric energy integration: Quantifying the value of design of markets for international transmission capacity." In: *Energy Economics* 40, pp. 760–772. DOI: 10.1016/j.eneco.2013.09.004.

Official Journal of the European Union (2019). *Regulation (EU) 2019/943 of the European Parliament and of the Council of 5 June 2019 on the internal market for electricity (recast)*. URL: http://data.europa.eu/eli/reg/2019/943/oj.

Papavasiliou, A. and S. S. Oren (2013). "Multiarea Stochastic Unit Commitment for High Wind Penetration in a Transmission Constrained Network." In: *Operations Research* 61.3, pp. 578–592. DOI: 10.1287/opre.2013.1174.

Pedregosa, F., G. Varoquaux, A. Gramfort, V. Michel, B. Thirion, O. Grisel, M. Blondel, P. Prettenhofer, R. Weiss, V. Dubourg, et al. (2011). "Scikit-learn: Machine learning in Python." In: *Journal of Machine Learning Research* 12, pp. 2825–2830. URL: http://www.jmlr.org/papers/volume12/pedregosa11a/pedregosa11a.pdf.

Plancke, G., C. De Jonghe, and R. Belmans (2016). "The implications of two German price zones in a european-wide context." In: *European Energy Market (EEM), 2016 13th International Conference on the*. IEEE, pp. 1–5. DOI: 10.1109/EEM.2016.7521290.

Powell, S. G. and S. S. Oren (1989). "The transition to nondepletable energy: social planning and market models of capacity expansion." In: *Operations Research* 37.3, pp. 373–383. DOI: 10.1287/opre.37.3.373.

Prognos (2013). *Entwicklung von Stromproduktionskosten: Die Rolle von Freiflächen-Solarkraftwerken in der Energiewende*. URL: http://www.prognos.com/uploads/tx_atwpubdb/131010_Prognos_Belectric_Studie_Freiflaechen_Solarkraftwerke_02.pdf.

Prognos and Fichtner (2013). *Kostensenkungspotenziale der Offshore-Windenergie in Deutschland*. URL: http://www.prognos.com/fileadmin/pdf/publikationsdatenbank/130822_Prognos_Fichtner_Studie_Offshore-Wind_Lang_de.pdf.

Stiftung Offshore-Windenergie (2015). *Übersicht Offshore Windparks Stand Juni 2015*. URL: https://www.offshore-stiftung.de/ausbau-verl%C3%A4uft-nach-plan-1765-megawatt-neu-am-netz.

Stigler, H. and C. Todem (2005). "Optimization of the Austrian electricity sector (Control Zone of VERBUND APG) by nodal pricing." In: *Central European Journal of Operations Research* 13.2, pp. 105–125. URL: https://search.proquest.com/docview/195552732?accountid=10755.

Stoft, S. (1997). "Transmission pricing zones: simple or complex?" In: *The Electricity Journal* 10.1, pp. 24–31. DOI: 10.1016/S1040-6190(97)80294-1.

TenneT (2015). *Statisches Netzmodell*. URL: https://web.archive.org/web/20150701215633/http://www.tennettso.de:80/site/binaries/content/assets/transparency/publications/static-grid-model/15_03_netzkarte.pdf.

THEMA Consulting Group (2013). *Loop flows- Final advice, prepared for The European Commission*. Tech. rep. URL: https://ec.europa.eu/energy/sites/ener/files/documents/201310_loop-flows_study.pdf.

Trepper, K., M. Bucksteeg, and C. Weber (2015). "Market splitting in Germany – New evidence from a three-stage numerical model of Europe." In: *Energy Policy* 87, pp. 199–215. DOI: 10.1016/j.enpol.2015.08.016.

van der Weijde, A. H. and B. F. Hobbs (2012). "The economics of planning electricity transmission to accommodate renewables: Using two-stage optimisation to evaluate flexibility and the cost of disregarding uncertainty." In: *Energy Economics* 34.6, pp. 2089–2101. DOI: 10.1016/j.eneco.2012.02.015.

VDE (2014). *FNN-Karte "Deutsches Höchstspannungsnetz 2014"*. URL: https://web.archive.org/web/20150117091305/http://www.vde.com:80/de/fnn/dokumente/documents/uebersichtsplan-2014.pdf.

Walras, L. (1900). *Èlements d'economie politique pure*. Lausanne, Paris.

Walton, S. and R. D. Tabors (1996). "Zonal transmission pricing: methodology and preliminary results from the WSCC." In: *The Electricity Journal* 9.9, pp. 34–41. DOI: 10.1016/S1040-6190(96)80456-8.

Wang, S., J. Zhu, L. Trinh, and J. Pan (Apr. 2008). "Economic assessment of HVDC project in deregulated energy markets." In: *2008 Third International Conference on Electric Utility Deregulation and Restructuring and Power Technologies*, pp. 18–23. DOI: 10.1109/DRPT.2008.4523373.

Zöttl, G. (2010). "A framework of peak load pricing with strategic firms." In: *Operations Research* 58.6, pp. 1637–1649. DOI: 10.1287/opre.1100.0836.

## Appendix A. Data Description

In this appendix, we provide detailed information on the data that we use in order to calibrate our model. Since we are looking at the hypothetical German electricity market in 2035 and the resulting investment incentives, we have to select all exogenous parameters based on future forecasts for this period. We consider the German market area since excellent data are available from the political processes that accompany the network expansion planning procedure. In order to ensure a high degree of consistency of the exogenous parameters—and in order to allow comparisons with other forecasts for that market area—we predominantly use input parameters from the *Network Development Plan Electricity* (NDP) which is the official basis for network expansion planning in Germany. Hereby, we mainly rely on the NDP 2030, where network expansion required until 2030 is determined, in its 2017 version. To be more specific, we use the regulator's approval of the scenario framework for the NDP 2030 (version 2017; cf. BNetzA (2016a)) and the Transmission System Operators' first draft of the NDP 2030 (version 2017; cf. German TSOs (2017)).

This scenario framework presents four scenarios. Three different RES development paths are considered and the generation mix is forecasted for 2030. Scenario B 2035 continues one of these development paths until 2035. This is the scenario we use for the calibration of our model's exogenous parameters.

We have chosen a scenario in the distant future for the following reasons: An investor considering an investment in generation capacity today must expect five to seven years, including the approval process and construction time, before the planned generator is operational. Thus, the period around 2025 would be around the beginning of the generator's

TABLE 5. Overview of nodes (federal states of Germany and neighboring countries) of the considered network according to the illustration in Figure 10.

| Node | Abbreviation |
|---|---|
| Federal states of Germany | |
| Baden-Wuerttemberg | BW |
| Bavaria | BY |
| Berlin | BE |
| Brandenburg | BB |
| Bremen | HB |
| Hamburg | HH |
| Hesse | HE |
| Lower Saxony | NI |
| Mecklenburg-Western Pomerania | MV |
| North Rhine-Westphalia | NW |
| Rhineland-Palatinate | RP |
| Saarland | SL |
| Saxony | SN |
| Saxony-Anhalt | ST |
| Schleswig-Holstein | SH |
| Thuringia | TH |
| Neighboring countries | |
| Austria | AT |
| Czech Republic | CZ |
| Denmark | DK |
| France | FR |
| Netherlands | NL |
| Poland | PL |
| Switzerland | CH |

lifetime. The average market conditions to be expected by the generator are better reflected by the conditions at a later date (here 2035). These are relevant for the investment decision. Another argument in favor of the use of scenario B 2035 is that a larger reduction in conventional generation capacity has taken place by then. As a result, more extensive generation capacity expansion is required, which allows for richer insights on the incentive mechanisms of various regulatory frameworks and the magnitude of the effects.

In the following we provide details on the data that we use to calibrate the network parameters, existing facilities, as well as cost and demand parameters.

A.1. **Existing Network.** Since our multilevel model computes optimal price zones, (long-term) investment incentives, and (short-term) production incentives in equilibrium, a significant simplification of the underlying network model is necessary in order to keep the calculations numerically tractable. Therefore, the German transmission network is aggregated so that each federal state is assigned a network node that serves the corresponding area of supply; see the illustration in Figure 10. An overview of all considered nodes is given in Table 5.

Since there is currently no single publicly available source for the calibration of the network with all relevant data for the model, the network infrastructure was calibrated using various sources. The existing lines between the federal states and their respective

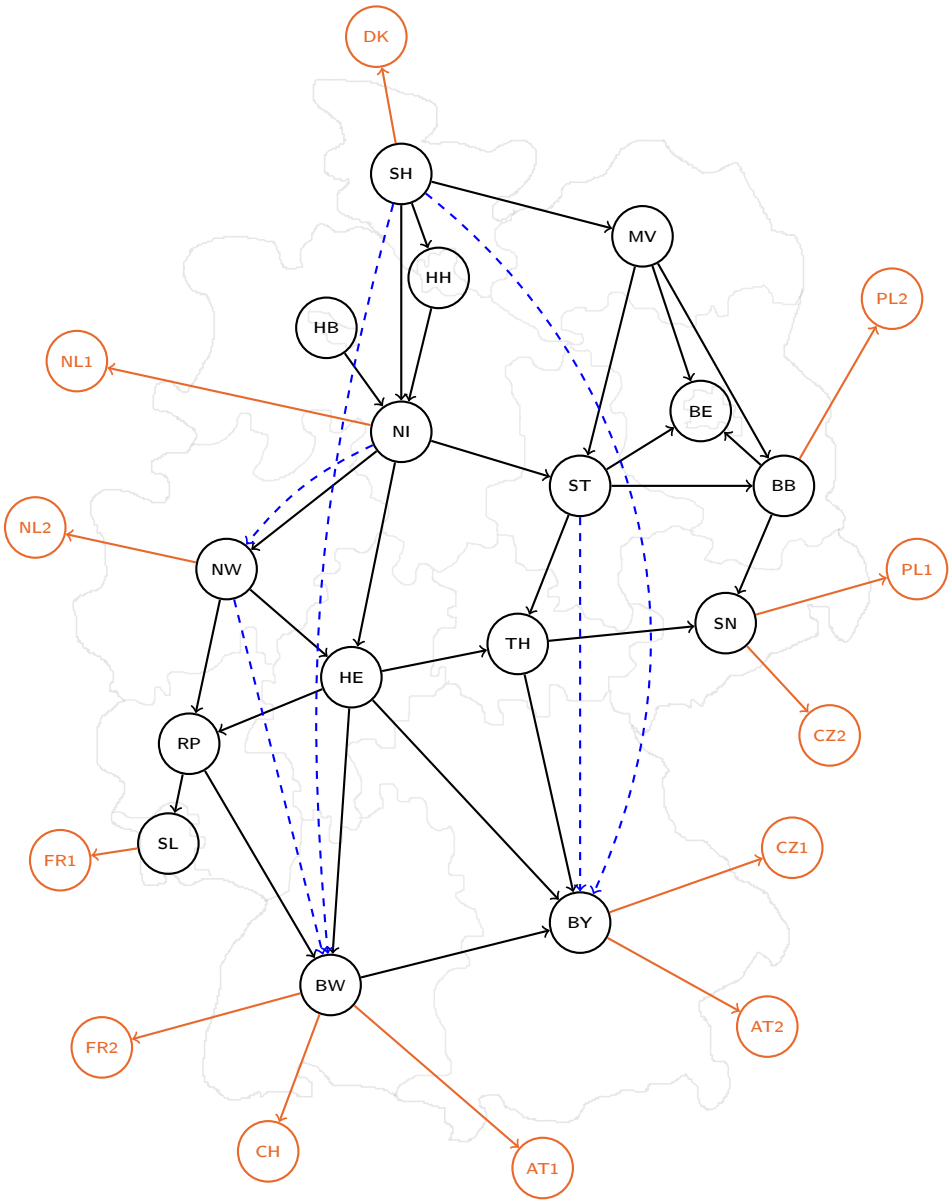


FIGURE 10. Network topology illustrating the considered nodes and lines. Orange: cross-border lines. Black: existing AC lines. Blue: candidate HVDC lines.

lengths are determined based on the map of the German extra-high voltage network by VDE (2014) as well as 50Hertz (2015), Amprion (2015), TenneT (2015), and the detailed network plan in Joost (2015). The relevant physical values such as reactance and thermal capacity of the different types of lines are listed in Kießling et al. (2001) and Egerer et al. (2014). In case there is more than one line between two nodes, these are aggregated to one line.

A.2. **Network Expansion.** In addition to the already existing transmission lines, we consider two different line expansion scenarios.

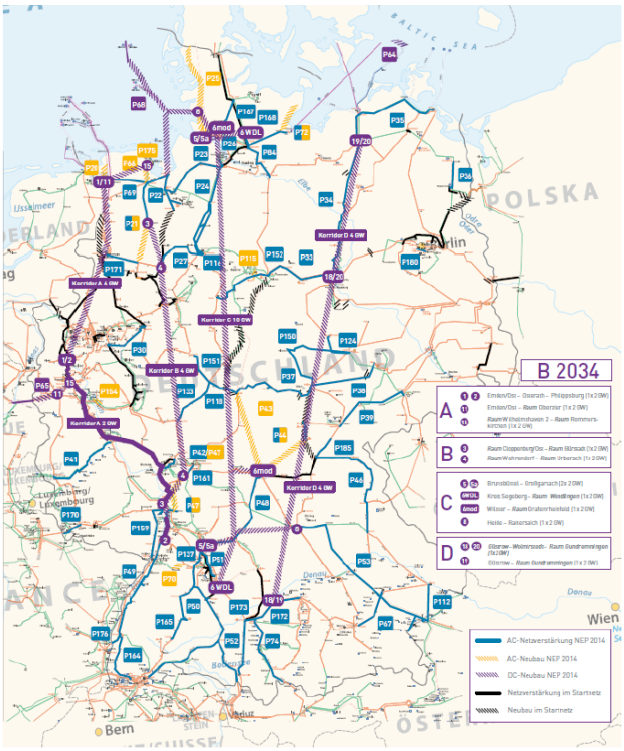


FIGURE 11. Network expansion measures of the NDP 2014, scenario B 2034. Source: German TSOs (2014a).

In the first scenario, transmission line expansion consists of the 15 HVDC transmission lines that have been proposed for the year 2034 in NDP 2014; cf. German TSOs (2014a). Line expansion takes place along four corridors for HVDC network expansion specified in German TSOs (2014a); see the new DC construction in Figure 11. Along each corridor, individual HVDC connections can be implemented as sub-projects of the NDP 2014.

In the second scenario, we consider line expansion by only five lines. This is motivated by the fact that the subsequent NDPs only consider a subset of the 15 HVDC connections. In German TSOs (2017), five transmission lines are evaluated as possible line candidates and turn out to be necessary for all possible scenarios of the year 2030. While German TSOs (2017) do not propose additional HVDC lines for the scenario of the year 2035, they validate that the HVDC lines proposed for 2030 will still be needed in 2035. These five transmission lines are assumed in our second line expansion scenario.

The remaining alternating current (AC) line candidates for expansion of the transmission network from German TSOs (2014a) are not taken into account. Since the investment costs of the neglected lines are far below the costs of the much longer HVDC lines and since many of these shorter lines run within a single federal state, the different incentive systems discussed here have a smaller effect on differences in the expansion of the AC lines than in the expansion decision of the HVDC lines.

Costs used for network expansion are based on cost estimates in German TSOs (2017). Current acceptance problems for the construction of HVDC lines in the affected regions have led to a further increase in network expansion costs. For the planned construction of DC underground cables (in order to address the concerns), 4 million € per km are estimated. In addition to a scenario with full cabling (100 % underground cable), German TSOs (2017) also examine a scenario with a cabling degree of 75 %. In this study, we consider the

TABLE 6. Costs of network expansion measures (specification of the respective line expansion projects) as annuities based on German TSOs (2014a) and German TSOs (2017).

| Start/end node | Measures according to NDP 2014 | Measures according to NDP 2030 (2017) | Investment cost (million € per year) |
|---|---|---|---|
| NI – NW | (A01, A11, A15) | (DC1) | 171.00 |
| NW – BW | (A02) | (DC2) | 162.00 |
| NI – HE | (B03, B04) | | 193.50 |
| SH – BW | (C05, C05a, C06WDL) | (DC3) | 298.00 |
| SH – BY | (C06mod, C08) | (DC4) | 274.50 |
| ST – BY | (D18, D19a) | (DC5) | 240.00 |
| MV – ST | (D19b, D20) | | 132.00 |

scenario with full cabling. DC converter stations, which are required twice per line, cost 0.20 million € per MW. For each line, the costs per km are multiplied by the respective line length, taking into account the DC converter stations at both ends. The annuity is calculated assuming an interest rate of 7 % and a depreciation period of 40 years.[5] Lines with the same start and end nodes are aggregated, using the average costs of the aggregated lines to compute line expansion costs for each of the two line expansion scenarios. Table 6 gives an overview of the costs of the network expansion measures used in the model.

A.3. **Demand.** Various development paths of net electricity consumption are taken into account in German TSOs (2017), p. 38. Different electricity demand drivers, in particular heat pumps and electro-mobility, as well as demand-reducing factors such as efficiency increases are taken into account. In previous versions of the NDP, it had been assumed that the opposing effects will largely cancel out each other. In contrast, German TSOs (2017) assume for the first time that the demand-increasing effects will dominate in three of the four scenarios, including scenario B 2035, and that electricity consumption will increase. Since the assumptions made have been controversially discussed during the approval process, cf. BNetzA (2016a), p. 103f., we assume a constant development of net electricity consumption. In our analysis, hourly demand data for Germany from 2014 are used, which are available at `https://www.entsoe.eu/data/power-stats/hourly_load/`. The allocation of demand to the federal states is based on statistical data of the "Länderarbeitskreis Energiebilanzen"; cf. German TSOs (2014b), p. 60, Table 32. Table 7 gives an overview of the electricity consumption in Germany by federal state per year.

A.4. **Renewable Production.** RES capacities are exogenous in our model. Thus, the expansion forecast of renewable generation capacity is included in the input data. For the calibration of the model, we use the particular expansion forecast of scenario B 2035, which provides corresponding data for wind onshore, wind offshore, and photovoltaics per federal state; see German TSOs (2017), p. 42, and Table 8.

The hourly fluctuating production of renewable energy generators per federal state is calculated using historical feed-in time series and high-resolution weather data. In order to take account of the different regional conditions for renewable energy generators within the federal states, five quality classes are determined for each federal state that allow limited capacities per class. The following data are used as sources for the technical potentials of the individual federal states: wind offshore from IWES (2012), wind onshore from BWE (2012), PV roof area from BMVI (2015), and PV open space data are derived from Destatis (2015). Depending on the quality class, the state-specific hourly feed-in vector is multiplied

[5]The depreciation period is based on the average operating life from Appendix 1 of StromNEV; see BGBl (2005).

TABLE 7. Electricity consumption by federal state based on German TSOs (2014b).

| Federal state | Consumption (TWh) | Share (%) |
|---|---|---|
| Baden-Wuerttemberg | 73.2 | 13.4 |
| Bavaria | 80.3 | 14.7 |
| Berlin | 13.4 | 2.4 |
| Brandenburg | 15.0 | 2.7 |
| Bremen | 5.0 | 0.9 |
| Hamburg | 12.7 | 2.3 |
| Hesse | 38.1 | 7.0 |
| Lower Saxony | 53.4 | 9.8 |
| Mecklenburg-Western Pomerania | 6.4 | 1.2 |
| North Rhine-Westphalia | 151.6 | 27.7 |
| Rhineland-Palatinate | 28.4 | 5.2 |
| Saarland | 9.2 | 1.7 |
| Saxony | 20.2 | 3.7 |
| Saxony-Anhalt | 15.7 | 2.9 |
| Schleswig-Holstein | 12.2 | 2.2 |
| Thuringia | 12.6 | 2.3 |
| Germany | 547.4 | 100.0 |

TABLE 8. Installed capacity of wind onshore, wind offshore, and photovoltaics by federal state. Existing capacity in 2014/2015 and forecast values of scenario B 2035 in GW based on German TSOs (2017), BNetzA (2015), and Stiftung Offshore-Windenergie (2015).

| | Wind onshore | | Wind offshore | | Photovoltaics | |
|---|---|---|---|---|---|---|
| Federal State | 2014 | B 2035 | 2015 | B 2035 | 2014 | B 2035 |
| Baden-Wuerttemberg | 0.6 | 2.3 | 0.0 | 0.0 | 5.0 | 10.7 |
| Bavaria | 1.4 | 2.4 | 0.0 | 0.0 | 11.1 | 18.2 |
| Berlin | 0.0 | 0.0 | 0.0 | 0.0 | 0.1 | 0.5 |
| Brandenburg | 5.4 | 7.4 | 0.0 | 0.0 | 2.9 | 4.2 |
| Bremen | 0.2 | 0.2 | 0.0 | 0.0 | 0.0 | 0.2 |
| Hamburg | 0.1 | 0.1 | 0.0 | 0.0 | 0.0 | 0.2 |
| Hesse | 1.1 | 2.3 | 0.0 | 0.0 | 1.8 | 4.1 |
| Lower Saxony | 7.9 | 12.7 | 2.1 | 10.9 | 3.5 | 7.9 |
| Mecklenburg-Western Pomerania | 2.6 | 5.1 | 0.3 | 4.6 | 1.3 | 2.4 |
| North Rhine-Westphalia | 3.7 | 6.0 | 0.0 | 0.0 | 4.2 | 10.6 |
| Rhineland-Palatinate | 2.7 | 4.2 | 0.0 | 0.0 | 1.9 | 4.1 |
| Saarland | 0.2 | 0.4 | 0.0 | 0.0 | 0.4 | 0.9 |
| Saxony | 1.1 | 2.1 | 0.0 | 0.0 | 1.6 | 3.0 |
| Saxony-Anhalt | 4.2 | 6.1 | 0.0 | 0.0 | 1.8 | 3.2 |
| Schleswig-Holstein | 4.9 | 8.0 | 1.4 | 3.5 | 1.5 | 2.9 |
| Thuringia | 1.2 | 2.5 | 0.0 | 0.0 | 1.1 | 2.2 |
| Germany | 37.3 | 61.8 | 3.8 | 19.0 | 38.2 | 75.3 |

TABLE 9. Feed-in from running water per federal state in 2013 based on BDEW (2015).

| Federal state | Feed-in (GWh) | Share (%) |
|---|---|---|
| Baden-Wuerttemberg | 5679.0 | 25.8 |
| Bavaria | 13 130.0 | 59.7 |
| Berlin | 0.0 | 0.0 |
| Brandenburg | 20.0 | 0.1 |
| Bremen | 42.0 | 0.2 |
| Hamburg | 0.0 | 0.0 |
| Hesse | 383.0 | 1.7 |
| Lower Saxony | 267.0 | 1.2 |
| Mecklenburg-Western Pomerania | 8.0 | 0.0 |
| North Rhine-Westphalia | 453.0 | 2.1 |
| Rhineland-Palatinate | 1260.0 | 5.7 |
| Saarland | 120.0 | 0.5 |
| Saxony | 314.0 | 1.4 |
| Saxony-Anhalt | 147.0 | 0.7 |
| Schleswig-Holstein | 6.0 | 0.0 |
| Thuringia | 147.0 | 0.7 |
| Germany | 21 976.0 | 100.0 |

by a quality factor. We assume that all five quality classes within a federal state have similar capacities. As a consequence, less productive sites of a federal state with a high RES potential are only built after more productive sites of an on average less productive federal state are filled. Forecasted capacities of scenario B 2035 are assigned to the classes according to the principles described above, i.e., the classes are filled to their maximum capacity in descending order starting with the best class.

Running water is integrated as an exogenously given hourly feed-in vector. In a first step, the monthly generation volumes for Germany from Destatis (2016b) are interpolated hourly. In a second step, hourly production is divided among the federal states according to the ratio of feed-in per federal state, as shown in Table 9.

A.5. **Existing Conventional Generators.** Based on the conditions outlined in BNetzA (2016a), this paper examines the investment incentives for conventional generators. Generation capacity that is installed in 2035 must therefore be included in the modeling. To this end, we use the data from BNetzA (2016a) and the corresponding generator list. There, all generators of the technology classes waste, lignite, natural gas, nuclear energy, mineral oil products, pumped storage, hard coal, etc. are listed with information on postal code, federal state, year of commissioning, and capacity; see the overview in Table 10. Our model is limited to the technologies hard coal, lignite, and natural gas, whereby natural gas plants are divided into combined cycle gas turbines (CCGT) and open gas turbine (GT) generators. In addition, market-led combined heat and power (CHP) generators coupled to CCGT generators are included in the modeling. Only existing generators that are still in operation in scenario B 2035 (i.e., with positive nominal power) and whose status is currently not "in planning" but "under construction", "in operation", "reserve", or "provisionally shut down" (if the scenario framework provides a capacity for 2035) are taken into account. Generation capacity investments in conventional technologies are always determined endogenously in the model. As a candidate for the analysis of the investment decision, investment in the CCGT technology can be made in any federal state without restrictions (coupled or not coupled with CHP). Note also that we allow for dismantling

TABLE 10. Net nominal power and projected net nominal power of all generation technologies for 2015 and for scenario B 2035 in GW. Source: German TSOs (2017), p. 26, Table 1.

| Generation technology | Reference 2015 | Scenario B 2035 |
|---|---|---|
| Nuclear energy | 10.80 | 0.00 |
| Lignite | 21.10 | 9.30 |
| Hard coal | 28.60 | 10.80 |
| Natural gas | 30.30 | 41.50 |
| Oil | 4.20 | 0.90 |
| Pump storage | 9.40 | 13.00 |
| Other conventional generation | 2.30 | 1.80 |
| Reserve capacity | 0.00 | 2.00 |
| Total conventional production | 106.90 | 79.30 |
| Wind onshore | 41.20 | 61.60 |
| Wind offshore | 3.40 | 19.00 |
| Photovoltaics | 39.30 | 75.30 |
| Biomass | 7.00 | 6.00 |
| Hydropower | 5.60 | 5.60 |
| Other renewable production | 1.30 | 1.30 |
| Total renewable production | 97.80 | 168.80 |

of lignite and hard coal generators, but not for investment in these technologies due to current efforts towards a coal phase-out in Germany; cf., e.g., Gerbaulet et al. (2012).

A.6. **CHP Generators.** When modeling CHP generators, a simplifying distinction is made between heat- and market-led CHP generators. Heat-led generators are integrated exogenously into the model by removing the existing capacities of heat-led CHP generators from the current generation capacities and integrating them into the model as an exogenously given feed-in vector. For simplicity, we assume a constant production quantity. Endogenous capacity extension is not possible.

In contrast, market-led CHP generators are considered endogenously. For this purpose, existing CHP generators coupled with CCGT are taken into account with lower marginal costs than CCGT generators without CHP in the existing generator park. These lower marginal costs arise due to additional income from the sale of heat. The marginal costs advantage for natural gas fired CHP generators is assumed at an annual average of 20 €/MWh; cf. EnCN/FAU/Prognos (2016), p. 40. This value roughly takes into account the value of the decoupled heat as a means of various CHP systems and operating modes occurring in practice. We assume a maximum installed capacity of 20 GW for natural gas CHP generators. Table 11 lists the existing CHP generators and capacity limits for each federal state, which are based on technical restrictions and heat demand. The limits assumed for the individual federal states cannot be used in total, as otherwise the maximum potential assumed for Germany would be exceeded.

A.7. **Investment Costs.** Since a representative year is considered in the model, investment costs are considered as annuities in the analysis of investment decisions. The values used for conventional electricity production are based on Konstantin (2013), pp. 306 as well as 310, and are given in Table 12. Since no further price changes are expected in the future for the investment and operational costs of conventional generators (except inflation), the current costs can also be used for the analysis of endogenous capacity expansions in 2035.

TABLE 11. Existing capacity of natural gas CHP generators in scenario B 2035 without generators with status "in planning" and maximum capacity expansions by federal state in MW based on the power plant list of the scenario framework for the NDP 2030 (version 2017). See BNetzA (2016b) for existing capacities and EnCN/FAU/Prognos (2016), p. 40, Table 9 for maximum capacity expansions.

| | existing CHP capacity | | Max. investment |
|---|---|---|---|
| Federal state | heat led | market led | market led |
| Baden-Wuerttemberg | 224 | 382 | 3000 |
| Bavaria | 585 | 684 | 1000 |
| Berlin | 0 | 744 | 1000 |
| Brandenburg | 86 | 118 | 500 |
| Bremen | 0 | 445 | 1000 |
| Hamburg | 16 | 127 | 1000 |
| Hesse | 489 | 169 | 1000 |
| Lower Saxony | 297 | 334 | 1000 |
| Mecklenburg-Western Pomerania | 53 | 251 | 500 |
| North Rhine-Westphalia | 1487 | 3152 | 4000 |
| Rhineland-Palatinate | 1017 | 422 | 1000 |
| Saarland | 0 | 114 | 500 |
| Saxony | 73 | 472 | 1000 |
| Saxony-Anhalt | 593 | 97 | 500 |
| Schleswig-Holstein | 0 | 75 | 1000 |
| Thuringia | 0 | 371 | 500 |
| Germany | 4919 | 7956 | limited to 7000 |

TABLE 12. Investment, operational, and variable production costs of conventional generators based on Konstantin (2013) and German TSOs (2017). ⋆The operational costs of lignite include the fixed operational costs of the lignite-fired power plants (52 000 €/MW) and the fixed costs of the opencast mine. Lignite-fired power plants must also generate contribution margins to the fixed costs of the opencast mine, which are assumed to be 49 500 €/MW. In total, this results in costs of 101 500 €/MW; cf. EnCN/FAU/Prognos (2016), p. 41.

| Technology | Investment cost (€/MW) | Operational cost (€/MW) | Fuel prices (€/MWh$_{\text{therm}}$) | Variable cost (€/MWh) |
|---|---|---|---|---|
| Lignite⋆ | 285 230 | 101 500 | 3.10 | 36.70–42.12 |
| Hard coal | 202 330 | 46 286 | 9.70 | 44.50–58.00 |
| CCGT | 80 100 | 16 500 | 30.00 | 58.18–70.62 |
| GT | 56 330 | 9333 | 30.00 | 93.42–121.37 |
| CCGT w. CHP | 94 392 | 16 500 | 30.00 | 38.18–50.95 |

The investment costs for renewable energies are based on Prognos (2013) and EnCN/FAU/Prognos (2016). Spatially differentiated investment costs are assumed for wind onshore in order to take into account the different conditions in the individual federal states. In order to achieve a certain amount of electricity per installed unit of wind, comparatively higher turbines with larger rotor diameters and thus more expensive turbines must be built

TABLE 13. Forecasted investment cost of renewable energies in 2035. Source: EnCN/FAU/Prognos (2016), p. 42, Table 11.

| Technology | Investment cost in 2035 (€/kW) | System configuration |
|---|---|---|
| Photovoltaics roof systems | 850 | Silicon-based DC-AC ratio of 1.20 |
| Photovoltaics open space systems | 600 | Silicon-based DC-AC ratio of 1.60 |
| Wind onshore 1 (HB, HH, MV, SH) | 1000 | Hub height 80 m 3 MW, 100 m rotor diameter |
| Wind onshore 2 (BB, BE, NI, NW, ST) | 1025 | Hub height 80 m 3 MW, 120 m rotor diameter |
| Wind onshore 3 (BW) | 1100 | Hub height 80 m 2.50 MW, 140 m rotor diameter |
| Wind onshore 4 (BY, HE, RP, SL, SN, TH) | 1075 | Hub height 80 m 2.50 MW, 130 m rotor diameter |
| Wind offshore | 2700 | Hub height 100 m 8 MW, 130 m rotor diameter |

in regions with lower wind than in strong wind areas. In the present analysis, there is a slight deviation from the approach of the NDP, where a reference installation of 3 MW is used; see German TSOs (2016), p. 54. For consistency reasons, the calculation of the utilization of the turbines for a hub height of 80 m is retained—even though this might be too low for the year 2035. A significantly higher hub height would lead to much more full-load hours compared to the NDP and thus reduce the comparability of the results between the NDP and this study. The assumptions regarding the system configurations together with the investment costs are shown in Table 13.

Regarding wind offshore, identical investment costs for wind turbines in the North Sea and the Baltic Sea are assumed for simplicity. In the Baltic Sea, lower water depths and coastal distances are compensated by more complex building structures due to poorer soil conditions. The underlying calculations for the development of investment costs, which is a continuation of the work of Prognos for the offshore wind industry, cf. Prognos and Fichtner (2013), are presented in EnCN/FAU/Prognos (2016).

For photovoltaics (PV), silicon-based systems are assumed both for open space and for roof systems. The cost assumptions were derived from AgoraEnergiewende (2015) and are given in EnCN/FAU/Prognos (2016). For all newly built PV systems in 2035, we assume investment costs for open space systems of 600 €/kW. The reason is that the renewable energy subsidy regimes, which are not examined in our study, are mainly suitable for controlling the investment in open space systems. Even with today's remuneration rates, roof systems are no longer profitable via the feed-in tariff and only become financially attractive in combination with other options, e.g., for capturing own consumption.

A.8. **Operational Costs.** In order to be able to take into account decisions on the dismantling of conventional generators, the annual operational costs, which consist of maintenance costs, personnel costs, insurance costs, and overheads, are considered for each technology. Like the investment costs, these values are based on Konstantin (2013).

A.9. **Variable Production Costs.** The variable production costs of conventional generators consist of fuel costs (see German TSOs (2017), p. 32, Table 3), costs for $CO_2$ emission certificates, and transport costs of fossil fuels. Note that the latter only play a role for hard coal and are determined for each federal state according to Figure 13 in Egerer et al.

(2014). For calibrating the variable costs of a certain generator, we have to consider its efficiency depending on technology and age as well as the emission factor of the respective technology, which is given in Table 34 on p. 62 in German TSOs (2014b). The prices of the $CO_2$ emission certificates under the European Emissions Trading System (EU ETS) are also taken from German TSOs (2017), and are assumed to be 33.00 €/t $CO_2$ in 2035.

Using the efficiency values per technology and decade of commissioning from Table 8 of Egerer et al. (2014), each generator of the generator list in BNetzA (2016a) can be assigned an efficiency level depending on the time of commissioning. Therefore, the variable production costs of generators of the same technology can vary considerably. In order to subsequently aggregate all generators of the same technology within a federal state, the respective net nominal powers are added. Variable production costs are calculated as the power-weighted average of the individual variable costs.

A.10. **Load Shedding, Interruptible Loads, and RES Curtailment.** If quantities traded at the spot market cannot be served physically even after redispatch, it is possible to switch on or off demand in order to obtain a feasible solution; cf. EnWG (2005), §13.2. To model the fact that load shedding is only carried out in case that generation redispatch does not suffice, we assume costs for positive and negative load shedding at the maximum of all variable costs. This ensures the correct order of generation redispatch and load shedding. Note that these costs are only used for calculation and are not included in welfare considerations, i.e., these costs are only used as penalties in the model's objective function and are not considered in our ex-post welfare analysis.

Renewables curtailment is possible at zero costs, which corresponds to the variable costs of renewable energy production.

A.11. **Neighboring Countries.** Hourly demand functions for electricity exports and imports of the neighboring countries are calibrated with the historical quantities traded across the border during the reference year 2014 and with the spot-market prices of the respective country. For DE, AT, CH, and FR we take these prices from http://www.epexspot.com/de/marktdaten/auktionshandel, for CZ from http://www.ote-cr.cz/statistics/yearly-market-report, for PL from http://wyniki.tge.pl/en/, and for DK from http://www.nordpoolspot.com/historical-market-data. Since the prices are not publicly available for the Netherlands (NL), the French prices are used as an estimate as both price patterns are very similar due to the close market coupling. The cross-border trading quantities are taken from ENTSO-E (2015).[6]

The data on transmission capacities to neighboring countries are not completely available from a single source and are partly contradictory. The modeling is essentially based on the map of VDE's German extra-high voltage grid (VDE 2014) and a list of existing interconnectors in Egerer et al. (2014), p. 37, Table 11. Lines currently not yet completed or planned are not considered in the modeling. The assumed line capacities are given in Table 14.

International trade takes place via explicit or implicit auctions, i.e., a separate market price is set for each country in periods with scarce transmission capacity (the so-called available transfer capacities, ATCs) between both countries; see also Table 14. The ATCs are determined for both directions as the maximum observed cross-border trading quantity. If there are two interconnectors from different federal states to the same country, the table shows the same ATC values for both, but on the spot market the sum of flows across all connections to the same country is limited by only one of the two values shown.

[6]Alternatively, the actual physical flows could be used. However, trading quantities provide a more precise picture of what is happening at the spot markets, whereas physical flows already include cross-border redispatch, loop flows of wind energy from northern Germany via neighboring countries to southern Germany and flows from trade in neighboring countries, e.g., between France and Switzerland.

TABLE 14. Thermal capacities and ATCs of considered cross-border interconnectors. Source: Egerer et al. (2014), ENTSO-E (2015), and VDE (2014). ⋆Denmark West is a zone within the price zones of Nord Pool. Denmark East is not connected to Germany in this model.

| From federal state | To neighboring country | Thermal capacity (MW) | Number of lines | ATC export (MW) | ATC import (MW) |
|---|---|---|---|---|---|
| BW | AT | 3504 | 4 | 0 | 0 |
| BW | FR | 3112 | 2 | 3025 | 1800 |
| BW | CH | 13 416 | 7 | 1375 | 3989 |
| BY | AT | 4888 | 8 | 0 | 0 |
| BY | CZ | 2720 | 2 | 1400 | 2798 |
| BB | PL | 784 | 1 | 2561 | 1700 |
| NI | NL | 2720 | 1 | 2561 | 1700 |
| NW | NL | 5440 | 3 | 2561 | 1700 |
| SN | CZ | 2720 | 1 | 1400 | 2798 |
| SN | PL | 2720 | 1 | 145 | 711 |
| SH | DK (West)⋆ | 3504 | 3 | 1500 | 1600 |
| SH | FR | 3112 | 2 | 3025 | 1800 |

Neither redispatch nor load shedding takes place abroad, i.e., all line congestion resulting from physical network restrictions must be resolved by appropriate measures within Germany.

A.12. **Trade Flows in the European Internal Market.** Since the German electricity market also needs to be designed to provide sufficient capacity for trade flows in the European internal market in the future, cf. German TSOs (2017), pp. 55–59, a transit through Germany from north-eastern Europe to south-western Europe is assumed in addition to the quantities traded in Germany and with its neighboring countries. To be specific, a transit with a constant hourly volume of 5.80 GWh through Germany is assumed in this study. The value is calculated as the hourly average of the predicted annual sum of transits through Germany given in German TSOs (2017), p. 59, Table 6, for scenario B 2035, which is 50.50 TWh. It is routed to Germany via three federal states in the north-east and exits Germany via three other federal states in the south-west; see Table 15. Transit flows do not respond to domestic German prices and are not taken into account for determining feasible cross-border flows via ATCs during spot-market trading between Germany and its neighboring countries. The reason for this is that some interconnectors are currently being expanded, particularly for these transit flows, which are not included in our existing network or in the calculation of ATCs. Examples are HVDC lines to Denmark, Norway, and Sweden.

[1]FRIEDRICH-ALEXANDER-UNIVERSITÄT ERLANGEN-NÜRNBERG, CHAIR OF ECONOMIC THEORY, LANGE GASSE 20, 90403 NÜRNBERG, GERMANY, [2]FRIEDRICH-ALEXANDER-UNIVERSITÄT ERLANGEN-NÜRNBERG, DISCRETE OPTIMIZATION, CAUERSTR. 11, 91058 ERLANGEN, GERMANY, [3]TRIER UNIVERSITY, DEPARTMENT OF MATHEMATICS, UNIVERSITÄTSRING 15, 54296 TRIER, GERMANY, [4]FRIEDRICH-ALEXANDER-UNIVERSITÄT ERLANGEN-NÜRNBERG, CHAIR OF REGULATION AND ENERGY MARKETS, LANGE GASSE 20, 90403 NÜRNBERG, GERMANY, [5]ENERGIE CAMPUS NÜRNBERG, FÜRTHER STR. 250, 90429 NÜRNBERG, GERMANY

TABLE 15. Transit flows through Germany as constant hourly flow from north-east to south-west in MWh based on German TSOs (2017).

| Federal state | Hourly import | Hourly export |
|---|---|---|
| Lower Saxony | 1800 | — |
| Mecklenburg-Western Pomerania | 1800 | — |
| Schleswig-Holstein | 1800 | — |
| Baden-Wuerttemberg | — | 1800 |
| Bavaria | — | 1800 |
| Rhineland-Palatinate | — | 1800 |